

NEUTRINO-MATTER INTERACTION RATES IN SUPERNOVAE

The Essential Microphysics of Core Collapse

Adam Burrows

Steward Observatory, The University of Arizona, Tucson, AZ 85721

burrows@zenith.as.arizona.edu

Todd A. Thompson*

Astronomy Department and Theoretical Astrophysics Center,

601 Campbell Hall, The University of California, Berkeley, CA 94720

thomp@astro.berkeley.edu

Abstract Neutrino-matter interaction rates are central to the core collapse phenomenon and, perhaps, to the viability of the mechanism of core-collapse supernova explosions. In this paper we catalog and discuss the major neutrino scattering, absorption, and production processes that together influence the outcome of core collapse and the cooling of protoneutron stars. These are the essential inputs into the codes used to simulate the supernova phenomenon and an understanding of these processes is a prerequisite to continuing progress in supernova theory.

Keywords: Supernovae, Neutrino Interactions, Neutrino Spectra, Protoneutron Stars, Kinetic Theory

1. Introduction

One of the key insights of the 20th Century was that most of the elements of nature are created by nuclear processes in stars. Supernova explosions are one major means by which these elements are injected into the interstellar medium and, hence, into subsequent generations of stars. Therefore, supernovae are central to the chemical evolution and progressive enrichment of the universe. Core-collapse supernova explo-

*Hubble Fellow

sions signal the death of a massive star and are some of the most majestic and awe-inspiring events in the cosmos. However, to fully understand the role of supernovae in the grand synthesis of creation, one must have a firm handle on the nuclear data. In particular, understanding the origin of iron-peak, r-process, and rp-process elements hinges upon improvements in our knowledge of the properties of exotic nuclei, some of which are far from the valley of beta stability.

The mechanism of core-collapse supernovae is thought to depend upon the transfer of energy from the core to the mantle of the inner regions of a massive star after it becomes unstable to collapse. Neutrinos seem to be the mediators of this energy transfer. In order to understand this coupling and the role of neutrinos in supernova explosions, one needs to master the particulars of the neutrino-matter scattering, production, and absorption rates. Since recently there has been some progress in understanding the associated microphysics, it is fitting to summarize the neutrino-matter cross sections and the production rates of neutrinos in the core-collapse context. To this end, we have assembled here a short précis of many of the relevant processes and physics. This contribution does not attempt to explain the hydrodynamics of supernova explosions, but does try to present the relevant neutrino processes that play a role. For the former, the reader is referred to Burrows, Hayes, and Fryxell (1995) and Burrows (2000).

In §2, we present a physical derivation of stimulated absorption (the Fermionic correlate to stimulated emission) and then in §3 we present the basic cross sections. In §4, we discuss the inelastic neutrino-electron and neutrino-nucleon scattering processes and energy redistribution. This is followed with a discussion of the alternate, more powerful formalism, for determining differential interaction rates in the many-body context and for handling redistribution, namely that of dynamical structure factors. Both the non-interacting and the interacting (in the context of a simple nuclear model) cases are explored, as well as collective excitations of the medium. Source terms for electron-positron annihilation (§6), neutrino-anti-neutrino annihilation (§7; Janka 1991), and nucleon-nucleon bremsstrahlung (§8) cap off our review of the major processes of relevance in core-collapse simulations. Nucleon–nucleon bremsstrahlung can compete with pair annihilation as a source for ν_μ , $\bar{\nu}_\mu$, ν_τ , and $\bar{\nu}_\tau$ neutrinos. Clearly, a mastery of these neutrino-matter processes is a prerequisite for progress in supernova theory and it is in that spirit that we have assembled this review.

2. Stimulated Absorption

The concept of stimulated emission for photons is well understood and studied, but the corresponding concept of stimulated *absorption* for neutrinos is not so well appreciated. This may be because its simple origin in Fermi blocking and the Pauli exclusion principle in the context of *net* emission is not often explained. The *net* emission of a neutrino is simply the difference between the emissivity and the absorption of the medium:

$$\mathcal{J}_{net} = \eta_\nu - \kappa_a I_\nu . \quad (1)$$

All absorption processes involving fermions will be inhibited by Pauli blocking due to final-state occupancy. Hence, η_ν in eq. (1) includes a blocking term, $(1 - \mathcal{F}_\nu)$ (Bruenn 1985). \mathcal{F}_ν is the invariant distribution function for the neutrino, whether or not it is in chemical equilibrium.

We can derive stimulated absorption using Fermi's Golden rule. For example, the net collision term for the process, $\nu_e n \leftrightarrow e^- p$, is:

$$\begin{aligned} \mathcal{C}_{\nu_e n \leftrightarrow e^- p} &= \int \frac{d^3 \vec{p}_{\nu_e}}{(2\pi)^3} \int \frac{d^3 \vec{p}_n}{(2\pi)^3} \int \frac{d^3 \vec{p}_p}{(2\pi)^3} \int \frac{d^3 \vec{p}_e}{(2\pi)^3} \left(\sum_s |\mathcal{M}|^2 \right) \\ &\times \Xi(\nu_e n \leftrightarrow e^- p) (2\pi)^4 \delta^4(\mathbf{p}_{\nu_e} + \mathbf{p}_n - \mathbf{p}_p - \mathbf{p}_e) , \quad (2) \end{aligned}$$

where \mathbf{p} is a four-vector and

$$\Xi(\nu_e n \leftrightarrow e^- p) = \mathcal{F}_{\nu_e} \mathcal{F}_n (1 - \mathcal{F}_e) (1 - \mathcal{F}_p) - \mathcal{F}_e \mathcal{F}_p (1 - \mathcal{F}_n) (1 - \mathcal{F}_{\nu_e}) . \quad (3)$$

The final-state blocking terms in eq. (3) are manifest, in particular that for the ν_e neutrino. Algebraic manipulations convert $\Xi(\nu_e n \leftrightarrow e^- p)$ in eq. (3) into:

$$\begin{aligned} \Xi(\nu_e n \leftrightarrow e^- p) &= \mathcal{F}_n (1 - \mathcal{F}_e) (1 - \mathcal{F}_p) \left[\frac{\mathcal{F}_{\nu_e}^{\text{eq}}}{1 - \mathcal{F}_{\nu_e}^{\text{eq}}} (1 - \mathcal{F}_{\nu_e}) - \mathcal{F}_{\nu_e} \right] \\ &= \frac{\mathcal{F}_n (1 - \mathcal{F}_e) (1 - \mathcal{F}_p)}{1 - \mathcal{F}_{\nu_e}^{\text{eq}}} [\mathcal{F}_{\nu_e}^{\text{eq}} - \mathcal{F}_{\nu_e}] , \quad (4) \end{aligned}$$

where

$$\mathcal{F}_{\nu_e}^{\text{eq}} = [e^{(\varepsilon_{\nu_e} - (\mu_e - \hat{\mu}))\beta} + 1]^{-1} \quad (5)$$

is an equilibrium distribution function for the ν_e neutrino and it has been assumed that only the electron, proton, and neutron are in thermal equilibrium. $\hat{\mu}$ is the difference between the neutron and the proton chemical potentials. Note that in $\mathcal{F}_{\nu_e}^{\text{eq}}$ there is no explicit reference to a neutrino chemical potential, though of course in beta equilibrium it is equal to $\mu_e - \hat{\mu}$. There is no need to construct or refer to a neutrino chemical potential in neutrino transfer.

We see that eq. (4) naturally leads to:

$$\mathcal{J}_{net} = \frac{\kappa_a}{1 - \mathcal{F}_\nu^{eq}} (B_\nu - I_\nu) = \kappa_a^* (B_\nu - I_\nu) . \quad (6)$$

Of course, B_ν is the black body function for neutrinos. This expression emphasizes the fact that $\mathcal{C}_{\nu_e n \leftrightarrow e^- p}$ and \mathcal{J}_{net} are the same entity. If neutrinos were bosons, we would have found a $(1 + \mathcal{F}_\nu^{eq})$ in the denominator, but the form of eq. (6) in which I_ν is manifestly driven to B_ν , the equilibrium intensity, would have been retained. From eqs. (4) and (6), we see that the stimulated absorption correction to κ_a is $1/(1 - \mathcal{F}_\nu^{eq})$. By writing the collision term in the form of eq. (6), with κ_a corrected for stimulated absorption, we have a net source term that clearly drives I_ν to equilibrium. The timescale is $1/c\kappa_a^*$. Though the derivation of the stimulated absorption correction we have provided here is for the $\nu_e n \leftrightarrow e^- p$ process, this correction is quite general and applies to all neutrino absorption opacities.

Kirchhoff's Law, expressing detailed balance, is:

$$\kappa_a = \eta_\nu / B_\nu \text{ or } \kappa_a^* = \eta'_\nu / B_\nu , \quad (7)$$

where η'_ν is not corrected for final-state neutrino blocking. Furthermore, the net emissivity can be written as the sum of its *spontaneous* and *induced* components:

$$\eta_\nu = \kappa_a \left[\frac{B_\nu}{1 \pm \mathcal{F}_\nu^{eq}} + \left(1 - \frac{1}{1 \pm \mathcal{F}_\nu^{eq}} \right) I_\nu \right] , \quad (8)$$

where $+$ or $-$ is used for bosons or fermions, respectively. Eq. (7) can be used to convert the absorption cross sections described in §3 into source terms.

3. Neutrino Cross Sections

Neutrino-matter cross sections, both for scattering and for absorption, play the central role in neutrino transport. The major processes are the super-allowed charged-current absorptions of ν_e and $\bar{\nu}_e$ neutrinos on free nucleons, neutral-current scattering off of free nucleons, alpha particles, and nuclei (Freedman 1974), neutrino-electron/positron scattering, neutrino-nucleus absorption, neutrino-neutrino scattering, neutrino-antineutrino absorption, and the inverses of various neutrino production processes such as nucleon-nucleon bremsstrahlung and the modified URCA process ($\nu_e + n + n \rightarrow e^- + p + n$). Compared with photon-matter interactions, neutrino-matter interactions are relatively simple functions of incident neutrino energy. Resonances play little or

no role and continuum processes dominate. Nice summaries of the various neutrino cross sections of relevance in supernova theory are given in Tubbs & Schramm (1975) and in Bruenn (1985). In particular, Bruenn (1985) discusses in detail neutrino–electron scattering and neutrino–antineutrino processes using the full energy redistribution formalism. He also provides a serviceable approximation to the neutrino–nucleus absorption cross section (Fuller 1980; Fuller, Fowler, & Newman 1982; Aufderheide et al. 1994). For a neutrino energy of ~ 10 MeV the ratio of the charged–current cross section to the ν_e –electron scattering cross section is ~ 100 . However, neutrino–electron scattering does play a role, along with neutrino–nucleon scattering and nucleon–nucleon bremsstrahlung, in the energy equilibration of emergent ν_μ neutrinos (Thompson, Burrows, & Horvath 2000).

Below, we list and discuss many of the absorption and elastic scattering cross sections one needs in detailed supernova calculations. In §4 and §5, we provide some straightforward formulae that can be used to properly handle inelastic scattering. The set of these processes comprises the essential microphysical package for the simulation of neutrino atmospheres and core–collapse supernovae.

3.1 $\nu_e + n \rightarrow e^- + p$:

The cross section per baryon for ν_e neutrino absorption on free neutrons is larger than that for any other process. Given the large abundance of free neutrons in protoneutron star atmospheres, this process is central to ν_e neutrino transport. A convenient reference neutrino cross section is σ_o , given by

$$\sigma_o = \frac{4G^2(m_e c^2)^2}{\pi(\hbar c)^4} \simeq 1.705 \times 10^{-44} \text{ cm}^2 . \quad (9)$$

The total $\nu_e - n$ absorption cross section is then given by

$$\sigma_{\nu_e n}^a = \sigma_o \left(\frac{1 + 3g_A^2}{4} \right) \left(\frac{\varepsilon_{\nu_e} + \Delta_{np}}{m_e c^2} \right)^2 \left[1 - \left(\frac{m_e c^2}{\varepsilon_{\nu_e} + \Delta_{np}} \right)^2 \right]^{1/2} W_M , \quad (10)$$

where g_A is the axial–vector coupling constant (~ -1.26), $\Delta_{np} = m_n c^2 - m_p c^2 = 1.29332$ MeV, and for a collision in which the electron gets all of the kinetic energy $\epsilon_{e^-} = \varepsilon_{\nu_e} + \Delta_{np}$. W_M is the correction for weak magnetism and recoil (Vogel 1984) and is approximately equal to $(1 + 1.1\varepsilon_{\nu_e}/m_n c^2)$. At $\varepsilon_{\nu_e} = 20$ MeV, this correction is only $\sim 2.5\%$. We include it here for symmetry’s sake, since the corresponding correction ($W_{\bar{M}}$) for $\bar{\nu}_e$ neutrino absorption on protons is $(1 - 7.1\varepsilon_{\bar{\nu}_e}/m_n c^2)$, which

at 20 MeV is a large -15% . To calculate κ_a^* , $\sigma_{\nu_e n}^a$ must be multiplied by the stimulated absorption correction, $1/(1 - \mathcal{F}'_{\nu_e})$, and final-state blocking by the electrons and the protons à la eq. (4) must be included.

3.2 $\bar{\nu}_e + p \rightarrow e^+ + n$:

The total $\bar{\nu}_e - p$ absorption cross section is given by

$$\sigma_{\bar{\nu}_e p}^a = \sigma_o \left(\frac{1 + 3g_A^2}{4} \right) \left(\frac{\epsilon_{\bar{\nu}_e} - \Delta_{np}}{m_e c^2} \right)^2 \left[1 - \left(\frac{m_e c^2}{\epsilon_{\bar{\nu}_e} - \Delta_{np}} \right)^2 \right]^{1/2} W_{\bar{M}}, \quad (11)$$

where $\epsilon_{e^+} = \epsilon_{\bar{\nu}_e} - \Delta_{np}$ and $W_{\bar{M}}$ is the weak magnetism/recoil correction given in §3.1. Note that $W_{\bar{M}}$ is as large as many other corrections and should not be ignored. To calculate κ_a^* , $\sigma_{\bar{\nu}_e p}^a$ must also be corrected for stimulated absorption and final-state blocking. However, the sign of $\mu_e - \hat{\mu}$ in the stimulated absorption correction for $\bar{\nu}_e$ neutrinos is flipped, as is the sign of μ_e in the positron blocking term. Hence, as a consequence of the severe electron lepton asymmetry in core-collapse supernovae, both coefficients are very close to one. Note that the $\bar{\nu}_e + p \rightarrow e^+ + n$ process dominates the supernova neutrino signal in proton-rich underground neutrino telescopes on Earth, such as Super Kamiokande, LVD, and MACRO, a fact that emphasizes the interesting complementarities between emission at the supernova and detection in Čerenkov and scintillation facilities.

3.3 $\nu_e A \leftrightarrow A' e^-$

From Bruenn (1985) the total $\nu_e - A$ absorption cross section, is approximated by

$$\sigma_A^a = \frac{\sigma_o}{14} g_A^2 N_p(Z) N_n(N) \left(\frac{\epsilon_\nu + Q'}{m_e c^2} \right)^2 \left[1 - \left(\frac{m_e c^2}{\epsilon_\nu + Q'} \right)^2 \right]^{1/2} W_{block}, \quad (12)$$

where $W_{block} = (1 - f_{e^-}) e^{(\mu_n - \mu_p - Q')\beta}$, $Q' = M_{A'} - M_A + \Delta \sim \mu_n - \mu_p + \Delta$, Δ is the energy of the neutron $1f_{5/2}$ state above the ground state and is taken to be 3 MeV (Fuller 1982), and the quantities $N_p(Z)$ and $N_n(N)$ are approximated by: $N_p(Z) = 0$, $Z - 20$, and 8 for $Z < 20$, $20 < Z < 28$, and $Z > 28$, respectively. $N_n(N) = 6$, $40 - N$, and 0 for $N < 34$, $43 < N < 40$, and $N > 40$, respectively. The opacity, corrected for stimulated absorption, is then

$$\kappa_a^* = X_H \rho N_A \sigma_A^a (1 - \mathcal{F}_{\nu_e}^{\text{eq}})^{-1}. \quad (13)$$

Since $N_n(N) = 0$ for $N > 40$, this absorption and emission process plays a role only during the very early phase of collapse. Typically at densities near $\rho \sim 10^{12} \text{ g cm}^{-3}$ $\kappa_a^* \rightarrow 0$.

3.4 $\nu_i + p \rightarrow \nu_i + p$:

The total $\nu_i - p$ scattering cross section for all neutrino species is:

$$\sigma_p = \frac{\sigma_o}{4} \left(\frac{\varepsilon_\nu}{m_e c^2} \right)^2 \left(4 \sin^4 \theta_W - 2 \sin^2 \theta_W + \frac{(1 + 3g_A^2)}{4} \right), \quad (14)$$

where θ_W is the Weinberg angle and $\sin^2 \theta_W \simeq 0.23$. In terms of $C'_V = 1/2 + 2 \sin^2 \theta_W$ and $C'_A = 1/2$, eq. (14) becomes (Schinder 1990):

$$\sigma_p = \frac{\sigma_o}{4} \left(\frac{\varepsilon_\nu}{m_e c^2} \right)^2 \left[(C'_V - 1)^2 + 3g_A^2 (C'_A - 1)^2 \right]. \quad (15)$$

The differential cross section is:

$$\frac{d\sigma_p}{d\Omega} = \frac{\sigma_p}{4\pi} (1 + \delta_p \mu), \quad (16)$$

where

$$\delta_p = \frac{(C'_V - 1)^2 - g_A^2 (C'_A - 1)^2}{(C'_V - 1)^2 + 3g_A^2 (C'_A - 1)^2}. \quad (17)$$

Note that δ_p , and δ_n below, are negative ($\delta_p \sim -0.2$ and $\delta_n \sim -0.1$) and, hence, that these processes are backward-peaked.

The transport (or momentum-transfer) cross section is simply

$$\sigma_p^{tr} = \frac{\sigma_o}{6} \left(\frac{\varepsilon_\nu}{m_e c^2} \right)^2 \left[(C'_V - 1)^2 + 5g_A^2 (C'_A - 1)^2 \right]. \quad (18)$$

where

$$\sigma_i^{tr} = \int \frac{d\sigma_i}{d\Omega} (1 - \mu) d\Omega = \sigma_i \left(1 - \frac{1}{3} \delta_i \right). \quad (19)$$

3.5 $\nu_i + n \rightarrow \nu_i + n$:

The total $\nu_i - n$ scattering cross section is:

$$\sigma_n = \frac{\sigma_o}{4} \left(\frac{\varepsilon_\nu}{m_e c^2} \right)^2 \left(\frac{1 + 3g_A^2}{4} \right). \quad (20)$$

The corresponding differential cross section is:

$$\frac{d\sigma_n}{d\Omega} = \frac{\sigma_n}{4\pi} (1 + \delta_n \mu), \quad (21)$$

where

$$\delta_n = \frac{1 - g_A^2}{1 + 3g_A^2}. \quad (22)$$

The transport cross section is

$$\sigma_n^{tr} = \frac{\sigma_o}{4} \left(\frac{\varepsilon_\nu}{m_e c^2} \right)^2 \left(\frac{1 + 5g_A^2}{6} \right). \quad (23)$$

The fact that δ_p and δ_n are negative and, as a consequence, that σ_i^{tr} is greater than σ_i increases the neutrino–matter energy coupling rate for a given neutrino flux in the semi-transparent region.

Horowitz (2002) has recently derived expressions that include a weak magnetism/recoil correction analogous to those previously discussed for the charged-current absorption rates $\nu_e n \leftrightarrow p e^-$ and $\bar{\nu}_e n \leftrightarrow n e^+$. We take the following form for the weak magnetism/recoil correction, a fit to the actual correction factor for the transport cross sections:

$$\sigma_{n,p}^{tr} \rightarrow \sigma_{n,p}^{tr} (1 + C_{WM} \varepsilon_\nu / m_{n,p}), \quad (24)$$

where, for neutrino-neutron scattering $C_{WM} \simeq -0.766$, for neutrino-proton scattering $C_{WM} \simeq -1.524$, for anti-neutrino-neutron scattering $C_{WM} \simeq -7.3656$, and for anti-neutrino-proton scattering $C_{WM} \simeq -6.874$.

In fact, neutrino-nucleon scattering is slightly inelastic and when this is germane, as with mu and tau neutrinos, the more general formalisms of §4.2 and §5 are necessary.

3.6 $\nu_i + A \rightarrow \nu_i + A$:

In the post-bounce phase, nuclei exist in the unshocked region exterior to the shock. At the high entropies in shocked protoneutron star atmospheres there are very few nuclei. There are alpha particles, but their fractional abundances are generally low, growing to interesting levels due to reassociation of free nucleons just interior to the shock only at late times. However, nuclei predominate on infall and neutrino-nucleus scattering (Freedman 1974) is the most important process during the lepton trapping phase.

The differential $\nu_i - A$ neutral-current scattering cross section may be expressed as:

$$\frac{d\sigma_A}{d\Omega} = \frac{\sigma_o}{64\pi} \left(\frac{\varepsilon_\nu}{m_e c^2} \right)^2 A^2 \{ \mathcal{W} \mathcal{C}_{FF} + \mathcal{C}_{LOS} \}^2 \langle \mathcal{S}_{ion} \rangle (1 + \mu), \quad (25)$$

where

$$\mathcal{W} = 1 - \frac{2Z}{A} (1 - 2 \sin^2 \theta_W), \quad (26)$$

Z is the atomic number, A is the atomic weight, and $\langle \mathcal{S}_{ion} \rangle$ is the ion-ion correlation function, determined mostly by the Coulomb interaction between the nuclei during infall. $\langle \mathcal{S}_{ion} \rangle$, in eq. (25) was investigated by Horowitz (1997) who approximated it with the expansion

$$\langle \mathcal{S}_{ion}(\epsilon) \rangle = \left[1 + \exp \left(- \sum_{i=0}^6 \beta_i(\Gamma) \epsilon^i \right) \right]^{-1}, \quad (27)$$

where

$$\Gamma = \frac{(Ze)^2}{a} \frac{1}{kT}, \quad \epsilon_i = \frac{\varepsilon_{\nu i}}{\hbar c a}, \quad a = \left(\frac{3}{4\pi n_{ion}} \right)^{1/3}, \quad (28)$$

a is the interparticle spacing, n_{ion} is the number density of ions, Γ is the ratio of Coulomb potential between ions to the thermal energy in the medium, and β_i are specified functions of Γ for each neutrino species.

Leinson et al. (1988) have investigated the electron polarization correction, \mathcal{C}_{LOS} , and find that

$$\mathcal{C}_{LOS} = \frac{Z}{A} \left(\frac{1 + 4 \sin^2 \theta_W}{1 + (kr_D)^2} \right), \quad (29)$$

where the Debye radius is

$$r_D = \sqrt{\frac{\pi \hbar^2 c}{4\alpha p_F E_F}}, \quad (30)$$

$k^2 = |\mathbf{p} - \mathbf{p}'|^2 = 2(\varepsilon_\nu/c)^2(1 - \mu)$, p_F and E_F are the electron Fermi momentum and energy, and α is the fine-structure constant ($\simeq 137^{-1}$). Note that $r_D \sim 10\hbar/p_F$ in the ultra-relativistic limit ($p_F \gg m_e c$). The \mathcal{C}_{LOS} term is important only for low neutrino energies, generally below ~ 5 MeV.

Following Tubbs & Schramm (1975) and Burrows, Mazurek, & Lattimer (1981), the form factor term, \mathcal{C}_{FF} , in eq. (25) can be approximated by:

$$\mathcal{C}_{FF} = e^{-y(1-\mu)/2}, \quad (31)$$

where

$$y = \frac{2}{3} \varepsilon_\nu^2 \langle r^2 \rangle / (\hbar c)^2 \simeq \left(\frac{\varepsilon_\nu}{56 \text{ MeV}} \right)^2 \left(\frac{A}{100} \right)^{2/3},$$

and $\langle r^2 \rangle^{1/2}$ is the *rms* radius of the nucleus. \mathcal{C}_{FF} differs from 1 for large A and ε_ν , when the de Broglie wavelength of the neutrino is smaller than the nuclear radius.

When $\langle \mathcal{S}_{ion} \rangle = \mathcal{C}_{FF} = \mathcal{C}_{LOS} + 1 = 1$, we have simple coherent Freedman scattering. The physics of the polarization, ion-ion correlation, and form factor corrections to coherent scattering is interesting in its own right, but has little effect on supernovae (Bruenn & Mezzacappa 1997). The total and transport scattering cross sections for $\nu_i - \alpha$ scattering ($Z = 2; A = 4$) are simply

$$\sigma_\alpha = \frac{3}{2} \sigma_\alpha^{tr} = 4 \sigma_o \left(\frac{\varepsilon_\nu}{m_e c^2} \right)^2 \sin^4 \theta_W. \quad (32)$$

4. Inelastic Neutrino Scattering

Many authors have studied inelastic neutrino-electron scattering as an important energy redistribution process which helps to thermalize neutrinos and increase their energetic coupling to matter in supernova explosions (Bruenn 1985; Mezzacappa & Bruenn 1993abc). Comparatively little attention has been paid to inelastic neutrino-nucleon scattering. Thompson, Burrows, & Horvath (2000) and Raffelt (2001) showed that, at least for mu and tau neutrinos, this process cannot be ignored. Here, we review the Legendre expansion formalism for approximating the angular dependence of the scattering kernel, detail our own implementation of scattering terms in the Boltzmann equation, and include a discussion of neutrino-nucleon energy redistribution. In §5, we present an alternate approach involving dynamical structure factors that is more easily generalized to include many-body effects.

The general collision integral for inelastic scattering may be written as

$$\mathcal{L}_\nu^{\text{scatt}}[f_\nu] = (1 - f_\nu) \int \frac{d^3 p'_\nu}{c(2\pi\hbar c)^3} f'_\nu R^{\text{in}}(\varepsilon_\nu, \varepsilon'_\nu, \cos \theta) \quad (33)$$

$$- f_\nu \int \frac{d^3 p'_\nu}{c(2\pi\hbar c)^3} (1 - f'_\nu) R^{\text{out}}(\varepsilon_\nu, \varepsilon'_\nu, \cos \theta) \quad (34)$$

$$= \tilde{\eta}_\nu^{\text{scatt}} - \tilde{\chi}_\nu^{\text{scatt}} f_\nu \quad (35)$$

where $\cos \theta$ is the cosine of the scattering angle, ε_ν is the incident neutrino energy, and ε'_ν is the scattered neutrino energy. Although we suppress it here, the incident and scattered neutrino phase space distribution functions (f_ν and f'_ν , respectively) have the following dependencies: $f_\nu = f_\nu(r, t, \mu, \varepsilon_\nu)$ and $f'_\nu = f'_\nu(r, t, \mu', \varepsilon'_\nu)$. μ and μ' are the cosines of the angular coordinate of the zenith angle in spherical symmetry and are related to $\cos \theta$ through

$$\cos \theta = \mu\mu' + [(1 - \mu^2)(1 - \mu'^2)]^{1/2} \cos(\phi - \phi'). \quad (36)$$

The only difference between f_ν and \mathcal{F}_ν in §2 is that here f_ν has explicit μ and ε_ν dependencies. R^{in} is the scattering kernel for scattering into the bin (ε_ν, μ) from any bin (ε'_ν, μ') and R^{out} is the scattering kernel for scattering out of the bin (ε_ν, μ) to any bin (ε'_ν, μ') . The kernels are Green functions that connect points in energy and momentum space. One may also write $R(\varepsilon_\nu, \varepsilon'_\nu, \cos \theta)$ as $R(q, \omega)$, where $\omega (= \varepsilon_\nu - \varepsilon'_\nu)$ is the energy transfer and $q (= [\varepsilon_\nu^2 + \varepsilon'_\nu{}^2 - 2\varepsilon_\nu \varepsilon'_\nu \cos \theta]^{1/2})$ is the momentum transfer, so that the kernel explicitly reflects these dependencies (§5).

An important simplification comes from detailed balance, a consequence of the fact that these scattering rates must drive the distribution to equilibrium. One obtains: $R^{\text{in}} = e^{-\beta\omega} R^{\text{out}}$, where $\beta = 1/T$. Therefore, we need deal only with R^{out} . The scattering kernels for inelastic neutrino-nucleon and neutrino-electron scattering depend in a complicated fashion on scattering angle. For this reason, one generally approximates the angular dependence of the scattering kernel with a truncated Legendre series (Bruenn 1985). We take

$$R^{\text{out}}(\varepsilon_\nu, \varepsilon'_\nu, \cos \theta) = \sum_{l=0}^{\infty} \frac{2l+1}{2} \Phi(\varepsilon_\nu, \varepsilon'_\nu, \cos \theta) P_l(\cos \theta), \quad (37)$$

where

$$\Phi_l(\varepsilon_\nu, \varepsilon'_\nu) = \int_{-1}^{+1} d(\cos \theta) R^{\text{out}}(\varepsilon_\nu, \varepsilon'_\nu, \cos \theta) P_l(\cos \theta). \quad (38)$$

In practice, one expands only to first order so that

$$R^{\text{out}}(\varepsilon_\nu, \varepsilon'_\nu, \cos \theta) \sim \frac{1}{2} \Phi_0(\varepsilon_\nu, \varepsilon'_\nu) + \frac{3}{2} \Phi_1(\varepsilon_\nu, \varepsilon'_\nu) \cos \theta. \quad (39)$$

Substituting into the first term on the right-hand-side of eq. (34) (the source) gives

$$\tilde{\eta}_\nu^{\text{scatt}} = (1-f_\nu) \int_0^\infty \frac{d\varepsilon'_\nu \varepsilon'_\nu{}^2}{c(2\pi\hbar c)^3} e^{-\beta\omega} \int_{-1}^{+1} d\mu' f'_\nu \int_0^{2\pi} d\phi' \left[\frac{1}{2} \Phi_0 + \frac{3}{2} \Phi_1 \cos \theta \right] \quad (40)$$

Substituting for $\cos \theta$ using eq. (36) and using the definitions

$$\tilde{J}_\nu = \frac{1}{2} \int_{-1}^{+1} d\mu f_\nu \quad (41)$$

and

$$\tilde{H}_\nu = \frac{1}{2} \int_{-1}^{+1} d\mu \mu f_\nu \quad (42)$$

we have that

$$\tilde{\eta}_\nu^{\text{scatt}} = (1-f_\nu) \frac{4\pi}{c(2\pi\hbar c)^3} \int_0^\infty d\varepsilon'_\nu \varepsilon'_\nu{}^2 e^{-\beta\omega} \left[\frac{1}{2} \Phi_0 \tilde{J}'_\nu + \frac{3}{2} \Phi_1 \mu \tilde{H}'_\nu \right]. \quad (43)$$

Integrating over μ to get the source for the zeroth moment of the transport equation,

$$\frac{1}{2} \int_{-1}^{+1} d\mu \tilde{\eta}_\nu^{\text{scatt}} = \frac{4\pi}{c(2\pi\hbar c)^3} \int_0^\infty d\varepsilon'_\nu \varepsilon'^2_\nu e^{-\beta\omega} \left[\frac{1}{2} \Phi_0 \tilde{J}'_\nu (1 - \tilde{J}_\nu) - \frac{3}{2} \Phi_1 \tilde{H}_\nu \tilde{H}'_\nu \right]. \quad (44)$$

Similarly, we may write the sink term of the Boltzmann equation collision term (second term in eq. 34), employing the Legendre expansion

$$\tilde{\chi}_\nu^{\text{scatt}} = \frac{4\pi}{c(2\pi\hbar c)^3} \int_0^\infty d\varepsilon'_\nu \varepsilon'^2_\nu \left[\frac{1}{2} \Phi_0 (1 - \tilde{J}'_\nu) - \frac{3}{2} \Phi_1 \mu \tilde{H}'_\nu \right]. \quad (45)$$

The contribution to the zeroth moment equation is then

$$\frac{1}{2} \int_{-1}^{+1} d\mu (-\tilde{\chi}_\nu^{\text{scatt}} f_\nu) = -\frac{4\pi}{c(2\pi\hbar c)^3} \int_0^\infty d\varepsilon'_\nu \varepsilon'^2_\nu \left[\frac{1}{2} \Phi_0 (1 - \tilde{J}'_\nu) \tilde{J}_\nu - \frac{3}{2} \Phi_1 \tilde{H}_\nu \tilde{H}'_\nu \right]. \quad (46)$$

Combining these equations, we find that

$$\begin{aligned} \frac{1}{2} \int_{-1}^{+1} d\mu \mathcal{L}_\nu^{\text{scatt}}[f_\nu] &= \frac{4\pi}{c(2\pi\hbar c)^3} \int_0^\infty d\varepsilon'_\nu \varepsilon'^2_\nu \\ &\times \left\{ \frac{1}{2} \Phi_0 \left[\tilde{J}'_\nu (1 - \tilde{J}_\nu) e^{-\beta\omega} - (1 - \tilde{J}'_\nu) \tilde{J}_\nu \right] - \frac{3}{2} \Phi_1 \tilde{H}_\nu \tilde{H}'_\nu (e^{-\beta\omega} - 1) \right\}. \end{aligned} \quad (47)$$

One can see immediately that including another term in the Legendre expansion (taking $R^{\text{out}} \sim (1/2)\Phi_0 + (3/2)\Phi_1 \cos\theta + (5/2)\Phi_2(1/2)(3\cos^2\theta - 1)$) necessitates including \tilde{P}_ν and \tilde{P}'_ν , the second angular moment of the neutrino phase-space distribution function, in the source and sink terms. While easily doable, we advocate retaining only the linear term and explore this approximation in the next two subsections.

4.1 Neutrino-Electron Scattering

The opacity due to neutrino-electron scattering can be large compared with that of other processes at low neutrino energies ($\varepsilon_\nu \lesssim 5$ MeV) and at high matter temperatures. A good approximation to the total scattering cross section has been derived by Bowers & Wilson (1982), which interpolates between analytic limits derived in Tubbs & Schramm (1975):

$$\sigma_e = \frac{3}{8} \sigma_o (m_e c^2)^{-2} \varepsilon_\nu \left(T + \frac{\mu_e}{4} \right) \left[(C_V + C_A)^2 + \frac{1}{3} (C_V - C_A)^2 \right], \quad (48)$$

where $C_V = 1/2 + 2 \sin^2 \theta_W$ for electron types, $C_V = -1/2 + 2 \sin^2 \theta_W$ for mu and tau neutrino types, $C_A = +1/2$ for ν_e and $\bar{\nu}_\mu$, and $C_A = -1/2$ for $\bar{\nu}_e$ and ν_μ .

However, the use of cross section (48) implicitly ignores the inelasticity of neutrino-electron scattering. When inelasticity is germane and a full energy redistribution formalism is needed, the scattering kernel approach of §4 in which different energy groups are coupled must be employed. The scattering kernel $R(\varepsilon_\nu, \varepsilon'_\nu, \cos \theta)$ in §4 is related to the fully relativistic structure function for neutrino-electron scattering:

$$R^{\text{out}}(\varepsilon_\nu, \varepsilon'_\nu, \cos \theta) = 2G^2 \frac{q_\mu^2}{\varepsilon'_\nu \varepsilon_\nu} [A\mathcal{S}_1(q, \omega) + \mathcal{S}_2(q, \omega) + B\mathcal{S}_3(q, \omega)] (1 - e^{-\beta\omega})^{-1}, \quad (49)$$

where $q_\mu (= (\omega, \vec{q}))$ is the four-momentum transfer, $A = (4\varepsilon_\nu \varepsilon'_\nu + q_\alpha^2)/2q^2$, $B = \varepsilon_\nu + \varepsilon'_\nu$, and $q_\alpha = (\varepsilon_\nu, \vec{q}_\nu)$. The relativistic structure functions (\mathcal{S}_i) are written in terms of the imaginary parts of the retarded polarization functions (Reddy, Prakash, & Lattimer 1998; Thompson, Burrows, & Horvath 2000; §5):

$$\mathcal{S}_1(q, \omega) = (\mathcal{V}^2 + \mathcal{A}^2) \left[\text{Im}\Pi_L^R(q, \omega) + \text{Im}\Pi_T^R(q, \omega) \right], \quad (50)$$

$$\mathcal{S}_2(q, \omega) = (\mathcal{V}^2 + \mathcal{A}^2) \text{Im}\Pi_T^R(q, \omega) - \mathcal{A}^2 \text{Im}\Pi_A^R(q, \omega), \quad (51)$$

and

$$\mathcal{S}_3(q, \omega) = 2\mathcal{V}\mathcal{A} \text{Im}\Pi_{VA}^R(q, \omega). \quad (52)$$

\mathcal{V} and \mathcal{A} are the appropriate vector and axial-vector coupling constants. Each of the polarization functions can be written in terms of one-dimensional integrals over electron energy (ε_e), which we label I_n (Reddy, Prakash, & Lattimer 1998)

$$\text{Im}\Pi_L^R(q, \omega) = \frac{q_\mu^2}{2\pi|q|^3} \left[I_2 + \omega I_1 + \frac{q_\mu^2}{4} I_0 \right], \quad (53)$$

$$\text{Im}\Pi_T^R(q, \omega) = \frac{q_\mu^2}{4\pi|q|^3} \left[I_2 + \omega I_1 + \left(\frac{q_\mu^2}{4} + \frac{q^2}{2} + m^2 \frac{q^2}{q_\mu^2} \right) I_0 \right], \quad (54)$$

$$\text{Im}\Pi_A^R(q, \omega) = \frac{m^2}{2\pi|q|} I_0, \quad (55)$$

and

$$\text{Im}\Pi_{VA}^R(q, \omega) = \frac{q_\mu^2}{8\pi|q|^3} [\omega I_0 + 2I_1]. \quad (56)$$

Reddy et al. (1998) were able to express the I_n 's in terms of polylogarithmic integrals such that

$$I_0 = Tz \left(1 - \frac{\xi_1}{z} \right), \quad (57)$$

$$I_1 = T^2 z \left(\eta_e - \frac{z}{2} - \frac{\xi_2}{z} - \frac{e_- \xi_1}{zT} \right), \quad (58)$$

and

$$I_2 = T^3 z \left(\eta_e^2 - z\eta_e + \frac{\pi^2}{3} + \frac{z^2}{3} + 2\frac{\xi_3}{z} - 2\frac{e_- \xi_2}{Tz} + \frac{e_-^2 \xi_1}{T^2 z} \right), \quad (59)$$

where $\eta_e = \mu_e/T$ is the electron degeneracy, $z = \beta\omega$, ω is the energy transfer, and

$$e_- = -\frac{\omega}{2} + \frac{q}{2} \sqrt{1 - 4\frac{m^2}{q_\mu^2}}. \quad (60)$$

In eqs. (57-59), the ξ_n 's are differences between polylogarithmic integrals; $\xi_n = \text{Li}_n(-\alpha_1) - \text{Li}_n(-\alpha_2)$, where

$$\text{Li}_n(y) = \int_0^y \frac{\text{Li}_{n-1}(x)}{x} dx, \quad (61)$$

and $\text{Li}_1(x) = \ln(1-x)$. The arguments necessary for computing the integrals are $\alpha_1 = \exp[\beta(e_- + \omega) - \eta_e]$ and $\alpha_2 = \exp(\beta e_- - \eta_e)$. Tables for computation of $\text{Li}_n(y)$ and the I_n s can be provided by Sanjay Reddy.

Figure (1) shows the full scattering kernel for $\varepsilon_\nu = 20$ MeV and $\varepsilon'_\nu = 2, 10, \text{ and } 16$ MeV as a function of the cosine of the scattering angle, $\cos \theta$. Note that although the absolute value of the energy transfer ($|\varepsilon_\nu - \varepsilon'_\nu|$) is the same for both $\varepsilon'_\nu = 16$ MeV and $\varepsilon'_\nu = 24$ MeV, the absolute value of $R^{\text{out}}(20, 16, \cos \theta)$ is more than twice that of $R^{\text{out}}(20, 24, \cos \theta)$, reflecting the fact that at this temperature the incoming neutrino is more likely to downscatter than upscatter. Figure (2) shows the scattering kernel for the same conditions as Fig. (1), but also includes both the first-order (short dashed lines) and second-order (long dashed lines) approximations to R^{out} . We generally employ the former. The latter is included to illustrate the improvement in including higher-order terms. In fact, the actual degree of expansion necessary to capture accurately the physics can only be ascertained by running full transport calculations. We have run dynamical simulations with only the zeroth-order and first-order terms in the Legendre expansion and find little or no difference between the emergent spectra and detailed thermodynamical evolution in the models we have studied. Smit (1998) and Smit & Cernohorsky (1995) have explored the importance of including the second-order term ($\propto \cos^2 \theta$, shown here) and find it negligible. The scattering-angle-averaged kernel, also the zeroth-order term in the Legendre series for R^{out} , is shown in Fig. (3) for ν_e -electron scattering for a matter temperature (T) of 6 MeV and with an electron degeneracy factor $\eta_e = \mu_e/T = 20$ as a function of ε'_ν for various incoming neutrino energies, ε_ν s.

In a full time-dependent simulation it is numerically costly to compute the Legendre moments of the scattering kernel ($\Phi_0(\varepsilon_\nu, \varepsilon'_\nu)$ and $\Phi_1(\varepsilon_\nu, \varepsilon'_\nu)$) via eq. (38) at each point in the computational domain. For this reason we tabulate $\Phi_0(\varepsilon_\nu, \varepsilon'_\nu)$ and $\Phi_1(\varepsilon_\nu, \varepsilon'_\nu)$ for each ε_ν and ε'_ν pair on a grid in temperature and η_e . Because the vector and axial-vector coupling constants for neutrino-electron scattering and the neutrino energy grouping differ between ν_e , $\bar{\nu}_e$, and ν_μ neutrinos, we construct separate tables for each species. Gauss-Legendre quadratures (16-point) are used to evaluate the angular integrals over $\cos\theta$ for $l = 0$ and $l = 1$ in eq. (38). At a given temperature/density/composition point the equation of state returns η_e and we then perform a six-point bivariate interpolation in T - η_e space, for the given ε_ν - ε'_ν combination, to obtain $\Phi_0(\varepsilon_\nu, \varepsilon'_\nu)$ and $\Phi_1(\varepsilon_\nu, \varepsilon'_\nu)$. The integrals over ε'_ν for each energy, which yield $\tilde{\eta}_\nu^{\text{scatt}}$ and $\tilde{\chi}_\nu^{\text{scatt}}$, are then computed using simple trapezoidal rule integration. In practice, we use 40 energy groups (n_f), 30 temperature points (N_T), and 30 η_e points (N_η). The tables are then $l \times n_f \times n'_f \times N_T \times N_\eta$ in size, with $l = 2$ (Φ_0 and Φ_1), or approximately 50 Megabytes. The source and sink at each energy ($\tilde{\eta}_\nu^{\text{scatt}}$ and $\tilde{\chi}_\nu^{\text{scatt}}$) are then included *explicitly* in a manner analogous to any of the emission or absorption processes. Using this method, our calculations including neutrino-electron scattering, are just 10-15% slower than our calculations ignoring this important equilibration process (Thompson, Burrows, & Pinto 2002).

This calculation of $\tilde{\eta}_\nu^{\text{scatt}}$ and $\tilde{\chi}_\nu^{\text{scatt}}$ uses only values of the neutrino energy density and flux from the previous timestep and, hence, we introduce an explicit timescale into the energy and electron fraction updates returned by our transport algorithm. For this reason, when the scattering rate is large we may encounter a numerical instability. Because the largest scattering rates are encountered when the neutrino phase-space distribution function is in local thermodynamical equilibrium and the scattering off electrons is unimportant, we simply divide the source and sink by a large factor (typically 100 above $\rho = 10^{14}$ g cm⁻³), thus circumventing the problem of introducing a short and explicit timescale. Again, because $f_\nu = f_\nu^{\text{eq}}$ at these high densities, this approximation is acceptable.

4.2 Neutrino-Nucleon Scattering

The kernel for inelastic neutrino-nucleon scattering can be related to the non-relativistic structure function employed in the thermalization studies of Thompson, Burrows, & Horvath (2000):

$$R^{\text{out}}(\varepsilon_\nu, \varepsilon'_\nu, \cos\theta) = G^2 S(q, \omega) [(1 + \cos\theta)V^2 + (3 - \cos\theta)A^2], \quad (62)$$

where $S(q, \omega)$ is given in terms of the imaginary part of the polarization function, analogous to neutrino-electron scattering (§4.1).

The neutrino-nucleon scattering kernels, while larger in absolute magnitude than the corresponding neutrino-electron scattering kernels are, at most points in energy space and thermodynamic space, much less broad. In fact, in thermodynamic regimes most relevant for the formation of the various species' spectra, the kernel is quite sharply peaked in energy. That is, for a given ε_ν the distribution of ε'_ν 's is tightly centered on ε_ν because the ratio of the neutrino energy to the nucleon mass is small. R^{out} as a function of $\cos\theta$, for neutrino-neutron scattering, is shown in Fig. (4) at a representative thermodynamic point. This plot is analogous to Fig. (1) for neutrino-electron scattering. By comparing the $\varepsilon'_\nu = 19$ MeV line with that for $\varepsilon'_\nu = 21$ MeV, one sees that the former is larger and, hence, downscattering is preferred. In addition, the overall magnitude is much larger than in the neutrino-electron scattering case. Figure (5) shows Φ_0 (eq. 38) for neutrino-neutron scattering as a function of ε'_ν for several ε_ν 's at the same thermodynamic point used in Fig. (3), the corresponding figure for neutrino-electron scattering. Note that while downscattering is strong for the $\varepsilon_\nu = 35$ MeV kernel, there is almost equal upscattering at $\varepsilon_\nu = 5$ MeV. In order to explore the effect of this process on the emergent spectra in dynamical simulations we must first deal with a technical problem.

In a typical simulation, we employ 40 energy groups for all neutrino species with $1 \text{ MeV} \leq \varepsilon_\nu \leq 320 \text{ MeV}$ for electron-type neutrinos and $1 \text{ MeV} \leq \varepsilon_\nu \leq 100 \text{ MeV}$ for anti-electron and muon neutrinos. The grouping is generally logarithmic for the ν_e s and linear for $\bar{\nu}_e$ and ν_μ . Neutrino-electron scattering and neutrino-nucleon scattering are most important as thermalization mechanisms at energies below ~ 60 MeV, where the phase space distribution of all neutrino species is largest. One can see clearly from Fig. (5) that a trapezoidal rule integration of Φ_0 over ε'_ν as it appears in eq. (44) and eq. (46) may grossly overestimate $\tilde{\eta}_\nu^{\text{scatt}}$ and $\tilde{\chi}_\nu^{\text{scatt}}$. In fact, with logarithmic energy grouping one may even calculate upscattering when there is none because the energy groups become larger with increasing energy.

For neutrino-electron scattering, we are able to employ a simple trapezoidal rule and adequately capture the qualities of the kernel. This implies that we use a linear interpolation for \tilde{J}'_ν and \tilde{H}'_ν in each energy bin. As Fig. (5) shows, however, in order to get an accurate integral over $\Phi_0(\varepsilon_\nu, \varepsilon'_\nu)$, we must do better than simple trapezoidal rule with linear interpolation. For neutrino-nucleon scattering, in order to increase the accuracy of our scheme without compromising computational efficiency, for a given energy grouping we pre-compute a grid of integrals over ε'_ν .

We assume that during the dynamical calculation and the computation of $\tilde{\eta}_\nu^{\text{scatt}}$ and $\tilde{\chi}_\nu^{\text{scatt}}$, both \tilde{J}'_ν and \tilde{H}'_ν are proportional to $A\varepsilon'_\nu + B$ over an energy interval $\varepsilon_{\nu,i} \leq \varepsilon'_\nu \leq \varepsilon_{\nu,i+1}$. Given this assumption and both $\Phi_0(\varepsilon_\nu, \varepsilon'_\nu)$ and $\Phi_1(\varepsilon_\nu, \varepsilon'_\nu)$ at a given T and $\eta_{n,p}$, we tabulate the following integrals:

$$\begin{aligned} & \int_{\varepsilon_{\nu,i}}^{\varepsilon_{\nu,i+1}} d\varepsilon'_\nu \varepsilon'^2_\nu \Phi_l(\varepsilon_\nu, \varepsilon'_\nu), \\ & \int_{\varepsilon_{\nu,i}}^{\varepsilon_{\nu,i+1}} d\varepsilon'_\nu \varepsilon'^2_\nu \varepsilon'_\nu \Phi_l(\varepsilon_\nu, \varepsilon'_\nu), \\ & \int_{\varepsilon_{\nu,i}}^{\varepsilon_{\nu,i+1}} d\varepsilon'_\nu \varepsilon'^2_\nu e^{-\beta\omega} \Phi_l(\varepsilon_\nu, \varepsilon'_\nu), \end{aligned}$$

and

$$\int_{\varepsilon_{\nu,i}}^{\varepsilon_{\nu,i+1}} d\varepsilon'_\nu \varepsilon'^2_\nu \varepsilon'_\nu e^{-\beta\omega} \Phi_l(\varepsilon_\nu, \varepsilon'_\nu),$$

where $l = 0, 1$ and each i is an individual energy group, set up at the beginning of the calculation. The integrals over ε'_ν are computed using 16-point Gauss-Legendre quadrature, each nested with another 16-point Gauss-Legendre quadrature for the integral over $\cos \theta$ necessary for each $\Phi_l(\varepsilon_\nu, \varepsilon'_\nu)$. These integrals are tabulated at 30 temperature and 30 $\eta_{n,p}$ points, analogous to the case for neutrino-electron scattering. For example, the integral

$$\begin{aligned} \int_0^\infty d\varepsilon'_\nu \varepsilon'^2_\nu \tilde{J}'_\nu \Phi_0(\varepsilon_\nu, \varepsilon'_\nu) &= \sum_{i=1}^{n_f} A_i \int_{\varepsilon_{\nu,i}}^{\varepsilon_{\nu,i+1}} d\varepsilon'_\nu \varepsilon'^2_\nu \varepsilon'_\nu \Phi_0(\varepsilon_\nu, \varepsilon'_\nu) \\ &+ \sum_{i=1}^{n_f} B_i \int_{\varepsilon_{\nu,i}}^{\varepsilon_{\nu,i+1}} d\varepsilon'_\nu \varepsilon'^2_\nu \Phi_0(\varepsilon_\nu, \varepsilon'_\nu), \quad (63) \end{aligned}$$

where $A_i = (\tilde{J}'_\nu - \tilde{J}'_\nu^{i+1})/(\varepsilon_\nu^{i'} - \varepsilon_\nu^{i+1'})$ and $B_i = \tilde{J}'_\nu - A_i \varepsilon_\nu^{i'}$. The total source and sink are given by integrals analogous to eq. (63) with appropriate changes to A_i and B_i , depending on if the term in the source or sink is over \tilde{J}'_ν or \tilde{H}'_ν . In practice, for a given temperature and density, we calculate the necessary integrals at the four nearest neighbor $T - \eta_{n,p}$ points saved in the table and then interpolate the solution using a four-point bivariate interpolation scheme. In this scheme, the energy integral over the kernel is reproduced extremely well and the primary uncertainty in calculating the total source and sink is due to the linear interpolation of \tilde{J}'_ν and \tilde{H}'_ν – the same as in the neutrino-electron scattering case. Also interesting is that because the neutrino-nucleon scattering kernel is so sharply peaked around ε_ν and drops off so quickly with ε'_ν , most terms in the sum in eq. (63) are zero. When we fill the

table, we note the index i of the lowest and highest $\varepsilon'_{\nu,i}$ intervals that contribute significantly (to a part in 10^4) to the total ε'_ν integral over Φ_l . Typically, only four to five energy groups must be included in the final sum. This decreases both the size of the table and the amount of time needed to calculate $\tilde{\eta}_\nu^{\text{scatt}}$ and $\tilde{\chi}_\nu^{\text{scatt}}$. Although the vector and axial-vector couplings for neutrino-neutron scattering are independent of neutrino species, we calculate separate tables for ν_e , $\bar{\nu}_e$, and ν_μ so as to allow for arbitrary energy grouping for each species.

The Elastic Limit: With the inelastic formalism in hand, it is instructive to construct the elastic limit. Note that in the limit of zero energy transfer, $S(q, \omega) \rightarrow S(0) = 2\pi n_{n,p} \delta(\omega)$, where $n_{n,p}$ is the neutron or proton number density (see eq. 80). The scattering term can then be written as

$$\begin{aligned} \mathcal{L}_{(0)}^{\text{scatt}}[f_\nu] &= (1 - f_\nu) \frac{C n_{n,p}}{c(2\pi\hbar c)^3} \int_0^\infty d\varepsilon'_\nu \varepsilon'^2_\nu e^{-\beta\omega} \delta(\omega) \int_{-1}^{+1} d\mu' f'_\nu \int_0^{2\pi} d\phi' M \\ &\quad - f_\nu \frac{C n_{n,p}}{c(2\pi\hbar c)^3} \int_0^\infty d\varepsilon'_\nu \varepsilon'^2_\nu \delta(\omega) \int_{-1}^{+1} d\mu' (1 - f'_\nu) \int_0^{2\pi} d\phi' M, \end{aligned} \quad (64)$$

where $M = [(1 + \cos\theta)V^2 + (3 - \cos\theta)A^2]$. Using eqs. (36), (41), and (42) we find that

$$\mathcal{L}_{(0)}^{\text{scatt}}[f_\nu] = \frac{4\pi C n_{n,p}}{c(2\pi\hbar c)^3} \int_0^\infty d\varepsilon'_\nu \varepsilon'^2_\nu \delta(\omega) [(1 - f_\nu) e^{-\beta\omega} \Xi_{\text{in}} - f_\nu \Xi_{\text{out}}], \quad (65)$$

where $\Xi_{\text{in}} = V^2(\tilde{J}'_\nu + \mu\tilde{H}'_\nu) + 3A^2(\tilde{J}'_\nu - \mu\tilde{H}'_\nu/3)$ and $\Xi_{\text{out}} = V^2(1 - \tilde{J}'_\nu - \mu\tilde{H}'_\nu) + 3A^2(1 - \tilde{J}'_\nu + \mu\tilde{H}'_\nu/3)$. Integrating over ε'_ν using the delta function, we have that

$$\begin{aligned} \mathcal{L}_{(0)}^{\text{scatt}}[f_\nu] &= 4\pi C \varepsilon_\nu^2 (V^2 + 3A^2) \left[(\tilde{J}_\nu - f_\nu) + \left(\frac{V^2 - A^2}{V^2 + 3A^2} \right) \mu \tilde{H}_\nu \right] \\ &= \sigma_{n,p} n_{n,p} \left[(\tilde{J}_\nu - f_\nu) + \delta_{n,p} \mu \tilde{H}_\nu \right] \end{aligned} \quad (66)$$

where $\sigma_{n,p} = (G^2/\pi c) \varepsilon_\nu^2 (V^2 + 3A^2)$, $\delta_{n,p}$ is the scattering asymmetry for neutrino-neutron or neutrino-proton scattering, G is the weak coupling constant, and c is the speed of light. The result presented in eq. (66) is to be compared with the full scattering part of the collision term:

$$-\kappa_s f_\nu + \frac{\kappa_s}{4\pi} \int \Phi(\boldsymbol{\Omega}, \boldsymbol{\Omega}') f_\nu(\boldsymbol{\Omega}') d\boldsymbol{\Omega}'. \quad (67)$$

Performing a first-order Legendre series expansion of the integral elastic scattering source term, and combining the scattering sink, $-\kappa_s f_\nu$,

with the scattering source, $\kappa_s \tilde{J}_\nu + \kappa_s \delta\mu \tilde{H}_\nu$, we obtain eq. (66) and an expression for $\delta_{n,p}$.

Note that taking the zeroth moment of $\mathcal{L}_{(0)}^{\text{scatt}}[f_\nu]$ yields zero, as it should in the elastic scattering limit. Further, note that the first moment is non-zero:

$$\begin{aligned} \frac{1}{2} \int_{-1}^{+1} d\mu \mu \mathcal{L}_{(0)}^{\text{scatt}}[f_\nu] &= \frac{G^2}{\pi c} n_{n,p} \varepsilon_\nu^2 \left[\frac{1}{3} \tilde{H}_\nu (V^2 - A^2) - \tilde{H}_\nu (V^2 + 3A^2) \right] \\ &= -\frac{G^2}{\pi c} n_{n,p} \varepsilon_\nu^2 \tilde{H}_\nu (V^2 + 3A^2) \left[1 - \frac{1}{3} \delta_{n,p} \right] \\ &= -\sigma_{n,p} n_{n,p} \tilde{H}_\nu \left[1 - \frac{1}{3} \delta_{n,p} \right]. \end{aligned} \quad (68)$$

This expression is to be compared with the elastic scattering momentum source term on the right-hand side of the first moment of the transport equation. In fact, the quantity $\sigma_{n,p} n_{n,p} (1 - \delta_{n,p}/3)$ defines the elastic transport cross section (see eq. 19).

5. Dynamic Structure Factors for Neutrino–Nucleon Interactions

An alternate formalism for handling inelastic neutrino-nucleon scattering that more straightforwardly than in §4.2 generalizes to include nucleon-nucleon correlations, whether due to fermi blocking or nuclear interactions, involves the dynamical structure factor $S(q, \omega)$. Our discussion here follows closely that found in Burrows and Sawyer (1998,1999). Recent explorations into the effects of many-body correlations on neutrino-matter opacities at high densities have revealed that for densities above $10^{14} \text{ gm cm}^{-3}$ both the charged-current and the neutral-current interaction rates are decreased by a factor of perhaps 2 to 3, depending on the density and the equation of state (Burrows & Sawyer 1998,1999; Reddy, Prakash, & Lattimer 1998; Yamada 1999). Furthermore, it has been shown that the rate of energy transfer due to neutral-current scattering off of nucleons exceeds that due to ν_μ -electron scattering (Janka et al. 1996; Thompson, Burrows, & Horvath 2000). Previously, it had been assumed that neutrino-nucleon scattering was elastic (Lamb & Pethick 1977). However, these recent reappraisals reveal that the product of the underestimated energy transfer per neutrino-nucleon scattering with cross section exceeds the corresponding quantity for neutrino-electron scattering. Since ν_e and $\bar{\nu}_e$ neutrinos participate in super-allowed charged-current absorptions on nucleons, neutrino-nucleon scattering has little effect on their rate of equilibration. However, such scattering is important for ν_μ and ν_τ equilibration. Since the many-

body correlation suppressions appear only above neutrinosphere densities ($\sim 10^{11} - 10^{13} \text{ gm cm}^{-3}$), it is only the kinematic effect, and not the interaction effect, that need be considered when studying the emergent spectra. In the following we adhere closely to the approach and formal development in Burrows and Sawyer (1998,1999). Without interactions, the relevant dynamical structure factor, $S(q, \omega)$, for neutrino–nucleon scattering is simply

$$S(q, \omega) = 2 \int \frac{d^3p}{(2\pi)^3} \mathcal{F}(|\mathbf{p}|) (1 - \mathcal{F}(|\mathbf{p} + \mathbf{q}|)) 2\pi \delta(\omega + \epsilon_{\mathbf{p}} - \epsilon_{\mathbf{p}+\mathbf{q}}), \quad (69)$$

where $\mathcal{F}(|\mathbf{p}|)$ is the nucleon Fermi–Dirac distribution function, $\epsilon_{\mathbf{p}}$ is the nucleon energy, ω is the energy transfer to the medium, and \mathbf{q} is the momentum transfer. The magnitude of \mathbf{q} is related to ω and E_1 , the incident neutrino energy, through the neutrino scattering angle, θ , by the expression (see text in §4 after eq. 36),

$$q = [E_1^2 + (E_1 - \omega)^2 - 2E_1(E_1 - \omega) \cos \theta]^{1/2}. \quad (70)$$

In the elastic limit and ignoring final–state nucleon blocking, $S(q, \omega) = 2\pi \delta(\omega) n_n$, the expected result, where n_n is the nucleon’s number density.

The neutral current scattering rate off of either neutrons or protons is (Burrows & Sawyer 1998),

$$\frac{d^2\Gamma}{d\omega d \cos \theta} = (4\pi^2)^{-1} G_W^2 (E_1 - \omega)^2 [1 - \mathcal{F}_\nu(E_1 - \omega)] \mathcal{I}_{\text{NC}}, \quad (71)$$

where

$$\mathcal{I}_{\text{NC}} = [(1 + \cos \theta)V + (3 - \cos \theta)A] S(q, \omega) \quad (72)$$

and

$$S(q, \omega) = 2\text{Im}\Pi^{(0)}(1 - e^{-\beta\omega})^{-1}. \quad (73)$$

V and A are the applicable vector and axial–vector coupling terms (see §3.4 and §3.5) and $\beta = 1/kT$. The free polarization function, $\Pi^{(0)}$, contains the full kinematics of the scattering, as well as blocking due to the final–state nucleon, and the relevant imaginary part of $\Pi^{(0)}$ is given by:

$$\text{Im}\Pi^{(0)}(q, \omega) = \frac{m^2}{2\pi q \beta} \log \left[\frac{1 + e^{-Q_+^2 + \beta\mu}}{1 + e^{-Q_+^2 + \beta\mu - \beta\omega}} \right], \quad (74)$$

where

$$Q_{\pm} = \left(\frac{m\beta}{2} \right)^{1/2} \left(\mp \frac{\omega}{q} + \frac{q}{2m} \right), \quad (75)$$

μ is the nucleon chemical potential, and m is the nucleon mass. The dynamical structure factor, $S(q, \omega)$, contains all of the information necessary to handle angular and energy redistribution due to scattering. The corresponding term on the right-hand-side of the transport equation is:

$$\mathcal{S}[\mathcal{F}_\nu] = (2\pi)^{-3} G_W^2 \int d^3 p'_\nu \mathcal{I}_{\text{NC}} \Xi_{SF} \quad (76)$$

where

$$\Xi_{SF} = [1 - \mathcal{F}_\nu(E_1)] \mathcal{F}'_\nu(E_1 - \omega) e^{-\beta\omega} - \mathcal{F}_\nu(E_1) [1 - \mathcal{F}'_\nu(E_1 - \omega)] \quad (77)$$

and p'_ν is the final state neutrino momentum.

In the non-degenerate nucleon limit, eq. (74) can be expanded to lowest order in Q_+^2 to obtain, using eq. (73), an approximation to the dynamical structure factor:

$$S(q, \omega) = \frac{n(2\pi m\beta)^{1/2}}{q} e^{-Q_+^2}, \quad (78)$$

where n is the nucleon number density. This says that for a given momentum transfer the dynamical structure factor is approximately a Gaussian in ω .

For charged-current absorption process, $\nu_e + n \rightarrow e^- + p$, $\text{Im}\Pi^{(0)}(q, \omega)$ is given by a similar expression:

$$\text{Im}\Pi^{(0)}(q, \omega) = \frac{m^2}{2\pi\beta q} \log \left[\frac{1 + e^{-Q_+^2 + \beta\mu_n}}{1 + e^{-Q_+^2 + \beta\mu_p - \beta\omega}} \right]. \quad (79)$$

Eq. (79) inserted into eq. (73) with a $(1 - e^{-\beta(\omega + \hat{\mu})})$, as is appropriate for the charged-current process, substituted for $(1 - e^{-\beta\omega})$, results in an expression that is a bit more general than the one employed to date by most practitioners (Bruenn 1985), *i.e.*, $S = (X_n - X_p)/(1 - e^{-\hat{\mu}/T})$. In the non-degenerate nucleon limit, the structure factor for the charged-current process can be approximated by eq. (78) with $n = n_n$. Note that for the structure factor of a charged-current interaction one must distinguish between the initial- and the final-state nucleons and, hence, between their chemical potentials. To obtain the structure factor for the $\bar{\nu}_e$ absorption process, one simply permutes μ_n and μ_p in eq. (79) and substitutes $-\hat{\mu}$ for $\hat{\mu}$ in the $(1 - e^{-\beta(\omega + \hat{\mu})})$ term.

In general, the widths of the structure factors are larger than might have been expected for scattering off of “heavy” particles. This is because in the past people thought that the neutrino could lose in ν -nucleon scattering an energy equal to only about $-E_1^2/m_n c^2$, *i.e.* that

the fractional energy lost is of order $p_\nu/m_n c$ ($\sim 1\%$). However, this assumes that the nucleons are stationary. In fact, they are thermal and, the fractional energy they can in a collision transfer to the neutrino is of order $p_n/m_n c$. Since the nucleons have such a large mass, if they and the neutrino have the same energy, $p_n/m_n c$ is much larger than $p_\nu/m_n c$, at incident neutrino energies of 10–30 MeV by as much as an order of magnitude. The formalism above incorporates the kinematics of such a collision, a realistic Fermi–Dirac energy distribution for the nucleons, and final–state nucleon blocking. The upshot is broad distributions. Including many–body effects further flattens and broadens the distribution, while lowering the central values of $d\sigma/d\omega$, as well as the total integral over ω (Burrows & Sawyer 1998,1999).

5.1 Aside: Static Structure Factors

In the limit of heavy nucleons, when we perform the integration in eq. (69) over a range of ω s and evaluated the inner factors at $\omega = 0$, we can express this limit as,

$$(2\pi)^{-1}S(q, \omega) \rightarrow (2\pi)^{-1}\delta(\omega) \int d\omega' S(q, \omega') \equiv \delta(\omega)S(q), \quad (80)$$

where $S(q)$ is the *static* structure factor. At the high densities and temperatures achieved in the supernova context, the $\omega = 0$ (elastic) limit is not particularly accurate (Burrows & Sawyer 1998; Reddy, Prakash, & Lattimer 1998).

$S(q)$ is merely the Fourier transform of the thermally–averaged density–density correlation function. This is the classic result that scattering off of a medium is in reality scattering off of the *fluctuations* in that medium. Also of interest is the long–wavelength limit, $q \rightarrow 0$, justified when the neutrino wavelength is much bigger than the interparticle separation. Statistical mechanics provides two useful and equivalent expressions for the long–wavelength limit, $S(0)$, the first (Landau & Lifschitz 1969) in terms of the isothermal compressibility of the medium $K_T (= -\frac{\partial \log V}{\partial P}|_T)$,

$$S(0) = \bar{n}^2 \beta^{-1} K_T = \bar{n} \frac{K_T}{K_0}, \quad (81)$$

where K_0 is the ideal gas compressibility and \bar{n} is the average nucleon density, and the second in terms of the derivative of the density with respect to the chemical potential of the nucleons, μ ,

$$S(0) = \beta^{-1} \frac{\partial \bar{n}}{\partial \mu}. \quad (82)$$

In the ideal gas limit of no correlation between particles, eqs. (81) and (82) show that $S(q)$ is simply equal to the number density, \bar{n} , as expected from eq. (69), without blocking. Eq. (81) reveals that if K_T is small because the matter is stiff, in the long-wavelength limit the neutrino-matter cross sections are *suppressed*. In general, when we acknowledge that the neutrino-matter interaction has axial-vector current and nucleon isospin terms, we require separate correlation functions for the neutron and the proton, as well as for spin correlations. These depend upon susceptibilities that are different from the compressibility, but we find suppression in these terms as well (Burrows & Sawyer 1998; Reddy, Prakash, & Lattimer 1998).

Eq. (82), equivalent to eq. (81) by a thermodynamic identity, is a powerful result of great generality. In standard approximation schemes for the many-body problem, the distribution function for a nucleon species is given by the Fermi-Dirac distribution in which the chemical potential μ is replaced by $\mu - v(\bar{n})$, where $v(\bar{n})$ is the average energy of interaction of the nucleon with the other nucleons and is a function of the density. Thus, the density is given implicitly by

$$\bar{n} = 2 \int \frac{d^3p}{(2\pi)^3} [1 + e^{\beta[(p^2/(2m) - \mu + v(\bar{n}))]}]^{-1}. \quad (83)$$

The expression (83) holds in the Hartree approximation; it holds in approaches that introduce mean meson fields instead of nuclear potentials; it holds in the Landau Fermi liquid theory (FLT), subject to the proviso that we use only results in which the derivative of the potential v (with respect to the \bar{n}) enters; and it holds in approaches using the Skyrme potential.

Differentiating (83), we can solve for $\frac{\partial \bar{n}}{\partial \mu}$ and $S(0)$,

$$S(0) = \beta^{-1} \frac{\partial \bar{n}}{\partial \mu} = h(\mu) [1 + h(\mu) \frac{\partial v}{\partial \bar{n}}]^{-1}, \quad (84)$$

where

$$h(\mu) = 2 \int \frac{d^3p}{(2\pi)^3} \frac{e^{\beta[p^2/(2m) - \mu + v]}}{[1 + e^{\beta[p^2/(2m) - \mu + v]}]^2} = 2 \int \frac{d^3p}{(2\pi)^3} \mathcal{F}(p) (1 - \mathcal{F}(p)) \quad (85)$$

and $\mathcal{F}(p)$ is the Fermi-Dirac function, but with the chemical potential displaced by v . If we regard particle densities as inputs to our calculations, then the displacement of the chemical potential by the nuclear potential is irrelevant, since the same difference, $\mu - v$, enters the calculation of the density in terms of the chemical potential. Thus, the

numerator of (84) contains no more than the familiar Pauli blocking effects (for the case $q = 0$); the denominator contains all of the effect of the interactions.

As an example, consider a two-nucleon potential $V(r)$. In the Hartree approximation, the average potential seen by a single nucleon is given by $v = \bar{n}U$, where $U = \int d^3x V(x)$, and (84) becomes

$$S(0) = h(\mu)[1 + h(\mu)U]^{-1}, \quad (86)$$

the potential providing an enhancement, if negative, and a suppression, if positive. The latter is the case for high-density nuclear matter.

5.2 Procedure for Calculating ν -nucleon Structure Functions for Neutral-Current Scattering Including Interactions

Now, taking only the neutron part of the vector-current coupling, the differential neutrino-nucleon scattering rate is given by,

$$\begin{aligned} \frac{d^2\Gamma}{d\omega d\cos\theta} = (4\pi^2)^{-1} G_W^2 E_2^2 [1 - f_\nu(E_2)] & \left[(1 + \cos\theta)(C_V^n)^2 S_{nn}(q, \omega) \right. \\ & \left. + (3 - \cos\theta)g_A^2 [S_{pp}^A(q, \omega) + S_{nn}^A(q, \omega) - 2S_{pn}^A(q, \omega)], \right] \quad (87) \end{aligned}$$

where $E_2 = E_1 - \omega$.

The structure functions, S (Fermi) and S^A (Gamow-Teller; axial), are elements of separate 2×2 symmetric matrices. For the vector dynamic structure function, S , we have

$$S(q, \omega) = \begin{pmatrix} S_{pp}(q, \omega) & S_{pn}(q, \omega) \\ S_{pn}(q, \omega) & S_{nn}(q, \omega) \end{pmatrix}.$$

The structure function matrix is given by,

$$S(q, \omega) = 2\text{Im} \left[\Pi^{(0)}(q, \omega) [1 - v(q)\Pi^{(0)}(q, \omega)]^{-1} \right] (1 - e^{-\beta\omega})^{-1} \quad (88)$$

where

$$\Pi^{(0)}(q, \omega) = \begin{pmatrix} \Pi_p^{(0)}(q, \omega) & 0 \\ 0 & \Pi_n^{(0)}(q, \omega) \end{pmatrix}$$

and $\Pi_p^{(0)}$ and $\Pi_n^{(0)}$ are given by the polarization function and evaluated with the proton and neutron chemical potentials, respectively (eq. 74). The potential matrix is,

$$v = \begin{pmatrix} v_1 + v_2 + 4\pi e^2(q^2 + q_{TF}^2)^{-1} & v_1 - v_2 \\ v_1 - v_2 & v_1 + v_2 \end{pmatrix},$$

where the v 's were defined in terms of Fermi liquid parameters and the term containing q_{TF} is the Thomas-Fermi screened Coulomb potential ($q_{TF}^2 = 4e^2\pi^{1/3}(3\bar{n}_p)^{2/3}$). Following Burrows and Sawyer (1998,1999) and for simplicity, we use here FLT and Landau parameters, in lieu of a more developed nuclear interaction model.

In a real calculation, in all the kinematic expressions the nucleon mass (m) is to be replaced by m^* . Unfortunately, the relation of Landau parameters to experimental results depends upon the effective mass in model-dependent ways. Taking $m^* = 0.75m_n$ as our fiducial value for the effective mass, we use parameters from Backman, Brown, & Niskanen (1985) and Brown and Rho (1981): $F_0 = -0.28$; $F'_0 = 0.95$; $G_0 = 0$; $G'_0 = 1.7$ and $\lambda = 2.63 \times 10^{-5} \text{MeV}^{-2}$, obtaining,

$$\begin{aligned} v_1 &= -7.4 \times 10^{-6} \text{MeV}^{-2} \\ v_2 &= 2.5 \times 10^{-5} \text{MeV}^{-2} \\ v_3 &= 0 \\ v_4 &= 4.5 \times 10^{-5} \text{MeV}^{-2}. \end{aligned} \tag{89}$$

For other values of the effective mass, we keep these potentials at the same value, which is to say we assume that the Landau parameters are proportional to m^*/m .

The form for the Gamow-Teller matrix, $S^A(q, \omega)$, is the same as that for S , except that the potential matrix is replaced by v^A

$$v^A = \begin{pmatrix} v_3 + v_4 & v_3 - v_4 \\ v_3 - v_4 & v_3 + v_4 \end{pmatrix}.$$

Taking the matrix inverses leads to the following forms for the combinations of structure functions that appear in (87)

$$S_{nn}(q, \omega) = 2\text{Im}[\Pi_n^{(0)} D_V^{-1}](1 - e^{-\beta\omega})^{-1}, \tag{90}$$

where

$$D_V = 1 - (v_1 + v_2)\Pi_n^{(0)} - (v_1 - v_2)^2\Pi_n^{(0)}\Pi_p^{(0)}Q_V^{-1}. \tag{91}$$

Q_V is given by the expression:

$$Q_V = 1 - 4\pi e^2(q^2 + q_{TF}^2)^{-1}\Pi_p^{(0)} - (v_1 + v_2)\Pi_p^{(0)}. \tag{92}$$

If, as in (89), we take $v_3 = 0$, we obtain the simple result for the axial-current terms,

$$S_A(q, \omega) = 2\text{Im}\left[\frac{\Pi_p^{(0)}(q, \omega) + \Pi_n^{(0)}(q, \omega)}{1 - v_4[\Pi_p^{(0)}(q, \omega) + \Pi_n^{(0)}(q, \omega)]}\right](1 - e^{-\beta\omega})^{-1}. \quad (93)$$

For the Fermi term, since $C_V^{(p)} = 1/2 - 2\sin^2\theta_W \sim 0$, we drop the proton structure function in (87). Furthermore, we use the potential parameters given in eq. (89), and in eq. (91) we drop the third term. This term would have been significant had it not been for the Coulomb term in the denominator, an illustration of the importance of the explicit inclusion of Coulomb forces, even for the neutron density correlations. Since the v_i s are all real, we obtain for the structure factors used in (87),

$$S_F(q, \omega) = 2\text{Im}\Pi_n^{(0)}(1 - e^{-\beta\omega})^{-1}\mathcal{C}_V^{-1}, \quad (94)$$

where

$$\mathcal{C}_V = (1 - v_F\text{Re}\Pi_n^{(0)})^2 + v_F^2(\text{Im}\Pi_n^{(0)})^2, \quad (95)$$

and

$$S_A(q, \omega) = 2\left[\text{Im}\Pi_p^{(0)}(q, \omega) + \text{Im}\Pi_n^{(0)}(q, \omega)\right](1 - e^{-\beta\omega})^{-1}\mathcal{C}_A^{-1}, \quad (96)$$

where

$$\mathcal{C}_A = \mathcal{C}_{A1} + \mathcal{C}_{A2}. \quad (97)$$

\mathcal{C}_{A1} and \mathcal{C}_{A2} are given by the expressions:

$$\mathcal{C}_{A1} = \left[1 - v_{GT}(\text{Re}\Pi_p^{(0)}(q, \omega) + \text{Re}\Pi_n^{(0)}(q, \omega))\right]^2 \quad (98)$$

and

$$\mathcal{C}_{A2} = v_{GT}^2\left[\text{Im}\Pi_p^{(0)}(q, \omega) + \text{Im}\Pi_n^{(0)}(q, \omega)\right]^2. \quad (99)$$

The F in $S_F(q, \omega)$ and the A in $S_A(q, \omega)$ stand for Fermi and Gamow-Teller (axial) and v_F and v_{GT} equal $(v_1 + v_2)$ and v_4 , respectively, in Fermi Liquid Theory. $S_A(q, \omega)$ in eq. (96) is now the entire axial term in eq. (87). $\mathcal{C}_{V,A}$ is the correction factor due to many-body effects for a given momentum transfer (or scattering angle) and energy transfer. A similar procedure is employed for calculating the many-body corrections to the charged-current rates (Burrows & Sawyer 1999).

5.3 Collective Excitations of the Medium

Following Burrows and Sawyer (1998,1999), we note that for most regions of phase space, \mathcal{C}_ν and \mathcal{C}_A in eqs. (95) and (97) are greater than one and represent suppression in the scattering rates. Their effects on the integrals over ω and θ are always suppressive. However, the terms containing the real parts have roots; these roots represent collective excitations. For the Fermi term, zero sound in the medium can be generated if the scattering has a (ω, q) pair that satisfies the mode's dispersion relation, *i.e.*, if it hits the resonance. Similarly, for the Gamow–Teller term, spin waves in the protons and the neutrons (related by a set phase) can be generated. These modes are the traveling–mode equivalents of the Gamow–Teller resonance in nuclei (a standing wave). The zero sound of the Fermi part is analogous to the Giant–Dipole resonance in nuclei. The resonances increase the structure function when the scattering transfer ratio, ω/q , equals the ratio of the collective excitation's angular frequency and wavenumber. For a given scattering angle, one can plot the differential cross section in ω and $\cos\theta$ as a function of ω/q to see the resonances. In Figure (6), we display this for five different angles between 15° and 180° , an incident neutrino energy of 20 MeV, a temperature of 5 MeV, a density of $3 \times 10^{14} \text{ g cm}^{-3}$, and an electron fraction, Y_e , of 0.3. We see in Figure 6 that the resonances in both the forward and the backward directions line up at the same values of ω/q , as expected for a collective mode, and we can straightforwardly calculate the mode's dispersion relation. This is akin to the Čerenkov effect. Note that the Gamow–Teller term dominates the Fermi term, so that in Figure 6 we are really seeing the spin waves related to the Gamow–Teller resonance. However, the dispersion relations for zero sound and these spin waves are generally similar. In fact, recalling the classic result of Fetter and Walecka (1971) that in the weak–coupling limit, the speed of zero sound in a degenerate system is $\sim v_{fermi}$, where v_{fermi} is the Fermi velocity, and recalling that for nucleons in nuclei v_{fermi} is $\sim 0.3c$, the calculated resonance value of ω/q is not unexpected. In Figure 7, we plot the Gamow–Teller structure function versus ω/q for various values of ω , m^* , and two values of the density. At $m^* = m_n$, for each value of the density we obtain a sharp resonance, but at two different speeds, reflecting the crude $\rho^{1/3}$ –dependence expected for v_{fermi} . For a given density, the mode speed is seen in Figure 7 to be inversely proportional to the effective mass. The width of the resonance is determined by the magnitude of the imaginary part of the polarization function.

6. e^+e^- Annihilation

Ignoring phase space blocking of neutrinos in the final state and taking the relativistic limit ($m_e \rightarrow 0$), the total electron–positron annihilation rate into neutrino–antineutrino pairs can be written in terms of the electron and positron phase space densities (Dicus 1972):

$$Q_{\nu_e\bar{\nu}_e} = K_i \left(\frac{1}{m_e c^2} \right)^2 \left(\frac{1}{\hbar c} \right)^6 \int \int \mathcal{F}_{e^-} \mathcal{F}_{e^+} (\varepsilon_{e^-}^4 \varepsilon_{e^+}^3 + \varepsilon_{e^-}^3 \varepsilon_{e^+}^4) d\varepsilon_{e^-} d\varepsilon_{e^+} , \quad (100)$$

where $K_i = (1/18\pi^4)c\sigma_o(C_V^2 + C_A^2)$. Again, $C_V = 1/2 + 2\sin^2\theta_W$ for electron types, $C_V = -1/2 + 2\sin^2\theta_W$ for mu and tau types, and $C_A^2 = (1/2)^2$. Rewriting eq. (100) in terms of the Fermi integral $F_n(\eta)$, we obtain:

$$Q_{\nu_e\bar{\nu}_e} = K_i (kT) \left(\frac{kT}{m_e c^2} \right)^2 \left(\frac{kT}{\hbar c} \right)^6 [F_4(\eta_e)F_3(-\eta_e) + F_4(-\eta_e)F_3(\eta_e)] , \quad (101)$$

where $\eta_e \equiv \mu_e/kT$ and

$$F_n(\eta) \equiv \int_0^\infty \frac{x^n}{e^{x-\eta} + 1} dx . \quad (102)$$

Integrating eq. (100), we obtain

$$Q_{\nu_e\bar{\nu}_e} \simeq 9.7615 \times 10^{24} \left[\frac{kT}{\text{MeV}} \right]^9 f(\eta_e) \text{ ergs cm}^{-3} \text{ s}^{-1} , \quad (103)$$

where

$$f(\eta_e) = \frac{F_4(\eta_e)F_3(-\eta_e) + F_4(-\eta_e)F_3(\eta_e)}{2F_4(0)F_3(0)} . \quad (104)$$

For $\nu_\mu\bar{\nu}_\mu$ and $\nu_\tau\bar{\nu}_\tau$ production combined,

$$Q_{\nu_{\mu,\tau}\bar{\nu}_{\mu,\tau}} \simeq 4.1724 \times 10^{24} \left[\frac{kT}{\text{MeV}} \right]^9 f(\eta_e) \text{ ergs cm}^{-3} \text{ s}^{-1} . \quad (105)$$

One can easily derive the spectrum of the total radiated neutrino energy (ε_T) by inserting a delta function ($\int \delta(\varepsilon_T - \varepsilon_{e^-} - \varepsilon_{e^+}) d\varepsilon_T$) into eq. (100). Recall that the total energy of the neutrinos in the final state is equal to the sum of the electron and positron energies in the initial state. Integrating first over ε_{e^+} to annihilate the delta function and then over ε_{e^-} to leave a function of ε_T , one obtains:

$$\frac{dQ}{d\varepsilon_T} = K_i \left(\frac{1}{m_e c^2} \right)^2 \left(\frac{1}{\hbar c} \right)^6 \int_0^{\varepsilon_T} \varepsilon_T (\varepsilon_T - \varepsilon_{e^-})^3 \varepsilon_{e^-}^3 \mathcal{F}_{e^-}[\varepsilon_{e^-}] \mathcal{F}_{e^+}[\varepsilon_T - \varepsilon_{e^-}] d\varepsilon_{e^-} . \quad (106)$$

The numerical evaluation of eq. (106) is straightforward. The average of ε_T is equal to:

$$\langle \varepsilon_T \rangle = \left(\frac{F_4(\eta_e)}{F_3(\eta_e)} + \frac{F_4(-\eta_e)}{F_3(-\eta_e)} \right) T, \quad (107)$$

which near $\eta_e \sim 0$ is $\sim 8T$ and for $\eta_e \gg 1$ is $\sim 4T(1 + \eta_e/5)$.

However, while the total energy loss rate (eq. 103) and the spectrum of ε_T pose no great mathematical problems, the production spectrum of an individual neutrino is not so easily reduced to a simple integral or to an analytic expression. This is due primarily to the awkward integration of the angular phase space terms, while subject to the momentum conservation delta function, and to the explicit dependence of the matrix elements on the electron/neutrino angles. From Dicus (1972), averaging over initial states and summing over final states, the matrix element for the $e^+e^- \rightarrow \nu\bar{\nu}$ process in the $m_e = 0$ limit is:

$$\frac{1}{4} \sum_s |\mathcal{M}|^2 = 16G^2 [(C_V + C_A)^2 \mathbf{p} \cdot \mathbf{q}_{\bar{\nu}} \mathbf{p}' \cdot \mathbf{q}_{\nu} + (C_V - C_A)^2 \mathbf{p} \cdot \mathbf{q}_{\nu} \mathbf{p}' \cdot \mathbf{q}_{\bar{\nu}}], \quad (108)$$

where p and p' are the four-momenta of the electron and positron, respectively, and q_{ν} and $q_{\bar{\nu}}$ are the four-momenta of the neutrino and antineutrino, respectively. Using the formalism of Bruenn (1985) and Fermi's Golden rule, expanding the production kernel in the traditional truncated Legendre series, performing the trivial angular integrals, taking the non-trivial angular integrals from Bruenn (1985), and ignoring final-state neutrino blocking, we obtain for the single-neutrino source spectrum due to e^+e^- annihilation:

$$\frac{dQ}{d\varepsilon_{\nu}} = \frac{8\pi^2}{(2\pi\hbar c)^6} \varepsilon_{\nu}^3 \int_0^{\infty} d\varepsilon_{\bar{\nu}} \varepsilon_{\bar{\nu}}^2 \Phi_0^p(\varepsilon_{\nu}, \varepsilon_{\bar{\nu}}), \quad (109)$$

where

$$\Phi_0^p(\varepsilon_{\nu}, \varepsilon_{\bar{\nu}}) = \frac{G^2}{\pi} \int_0^{\varepsilon_{\nu} + \varepsilon_{\bar{\nu}}} d\varepsilon_{e^-} \mathcal{F}_{e^-}[\varepsilon_{e^-}] \mathcal{F}_{e^+}[\varepsilon_{\nu} + \varepsilon_{\bar{\nu}} - \varepsilon_{e^-}] H_0(\varepsilon_{\nu}, \varepsilon_{\bar{\nu}}, \varepsilon_{e^-}), \quad (110)$$

and

$$H_0(\varepsilon_{\nu}, \varepsilon_{\bar{\nu}}, \varepsilon_{e^-}) = (C_V + C_A)^2 J_0^I(\varepsilon_{\nu}, \varepsilon_{\bar{\nu}}, \varepsilon_{e^-}) + (C_V - C_A)^2 J_0^{II}(\varepsilon_{\nu}, \varepsilon_{\bar{\nu}}, \varepsilon_{e^-}). \quad (111)$$

The J_0 s in eq. (111) come from the more obdurate angular integrals required by the dot products in eq. (108) and the momentum delta function and have the symmetry:

$$J_0^I(\varepsilon_{\nu}, \varepsilon_{\bar{\nu}}, \varepsilon_{e^-}) = J_0^{II}(\varepsilon_{\bar{\nu}}, \varepsilon_{\nu}, \varepsilon_{e^-}). \quad (112)$$

From eqs. (109) and (111), we see that the differences between the spectra of the ν_e and ν_μ neutrinos flow solely from their correspondingly different values of $(C_V + C_A)^2$ and $(C_V - C_A)^2$. One can use 4-point Gauss–Legendre integration to calculate eq. (110) and 16-point Gauss–Laguerre integration to calculate eq. (109).

At small η_e , the e^+e^- annihilation spectra and total energy loss rates for the ν_e and $\bar{\nu}_e$ neutrinos are similar, as are the average emitted ν_e and $\bar{\nu}_e$ neutrino energies. However, as η_e increases, both the total energy radiated in $\bar{\nu}_e$ neutrinos and the average $\bar{\nu}_e$ energy start to lag the corresponding quantities for the ν_e neutrinos. This is true despite the fact that the total number of ν_e and $\bar{\nu}_e$ neutrinos radiated is the same. If final-state blocking is ignored, $\langle \varepsilon_i \rangle / T$ is a function of η_e alone, becoming linear with η_e at high η_e and one half of eq. (107) (~ 4.0) at low η_e . Note also that $\langle \varepsilon_{\nu_\mu} \rangle / T$ and $\langle \varepsilon_{\bar{\nu}_\mu} \rangle / T$ are closer to one another than are $\langle \varepsilon_{\nu_e} \rangle / T$ and $\langle \varepsilon_{\bar{\nu}_e} \rangle / T$. The individual production spectra vary in peak strength, in peak energy, and in low-energy shape, but they are quite similar on the high-energy tail. Due to the parity-violating matrix element for the $e^+e^- \rightarrow \nu\bar{\nu}$ process and the fact that η_e is positive, the antineutrino spectra of all species are softer than the neutrino spectra. The pair sums of the integrals under these curves are given by eqs. (103) and (105). For $\eta_e = 0$, 50% of the pair energy emission of electron types is in $\bar{\nu}_e$ neutrinos, but at $\eta_e = 10$ only 42% of this total energy is in $\bar{\nu}_e$ neutrinos. However, at $\eta_e = 10$, the $\bar{\nu}_\mu$ neutrinos still constitute 48.5% of the $\nu_\mu/\bar{\nu}_\mu$ pair emission. These differences reflect differences in the corresponding coupling constants C_V and C_A .

7. $\nu_i\bar{\nu}_i$ Annihilation

In the limit of high temperatures and ignoring electron phase space blocking, the $\nu_i\bar{\nu}_i$ annihilation rate into e^+e^- pairs can be written (Janka 1991):

$$Q_{\nu_i\bar{\nu}_i} = 4K_i\pi^4 \left(\frac{1}{m_e c^2} \right) \left(\frac{4\pi}{c} \right)^2 \int \int \Phi' J_{\nu_i} J_{\bar{\nu}_i} (\varepsilon_{\nu_i} + \varepsilon_{\bar{\nu}_i}) d\varepsilon_{\nu_i} d\varepsilon_{\bar{\nu}_i}, \quad (113)$$

where J_ν is the zeroth moment of the radiation field, ε_ν is the neutrino energy, K_i is defined as before (*i.e.*, $K_i = (1/18\pi^4)c\sigma_o(C_V^2 + C_A^2)$), and

$$\Phi'(\langle \mu_{\nu_i} \rangle, \langle \mu_{\bar{\nu}_i} \rangle, p_{\nu_i}, p_{\bar{\nu}_i}) = \frac{3}{4} \left[1 - 2\langle \mu_{\nu_i} \rangle \langle \mu_{\bar{\nu}_i} \rangle + p_{\nu_i} p_{\bar{\nu}_i} + \frac{1}{2}(1 - p_{\nu_i})(1 - p_{\bar{\nu}_i}) \right], \quad (114)$$

where the flux factor $\langle \mu_{\nu_i} \rangle = H_\nu / J_\nu$ and the Eddington factor $p_\nu = \langle \mu_{\nu_i}^2 \rangle = P_\nu / J_\nu$. Eq. (113) can be rewritten in terms of the invariant

distribution functions \mathcal{F}_ν :

$$Q_{\nu_i\bar{\nu}_i} = K_i \left(\frac{1}{m_e c^2} \right)^2 \left(\frac{1}{\hbar c} \right)^6 \int \int \Phi' \mathcal{F}_{\nu_i} \mathcal{F}_{\bar{\nu}_i} (\varepsilon_{\nu_i}^4 \varepsilon_{\bar{\nu}_i}^3 + \varepsilon_{\nu_i}^3 \varepsilon_{\bar{\nu}_i}^4) d\varepsilon_{\nu_i} d\varepsilon_{\bar{\nu}_i}. \quad (115)$$

Note that when the radiation field is isotropic ($\Phi' = 1$) and when $\eta_e = 0$ the total rate for e^+e^- annihilation given in eq. (100) equals that for $\nu_i\bar{\nu}_i$ annihilation given in eq. (115), as expected. Buras et al. (2002) have addressed the related and interesting process of $\nu_i\bar{\nu}_i \rightarrow \nu_j\bar{\nu}_j$. We refer to that paper for a discussion of the relevance and rates of this process.

8. Nucleon–Nucleon Bremsstrahlung

A production process for neutrino/anti-neutrino pairs that has recently received attention in the supernova context is neutral-current nucleon–nucleon bremsstrahlung ($n_1 + n_2 \rightarrow n_3 + n_4 + \nu\bar{\nu}$). Its importance in the cooling of old neutron stars, for which the nucleons are quite degenerate, has been recognized for years (Flowers 1975), but only in the last few years has it been studied for its potential importance in the quasi-degenerate to non-degenerate atmospheres of protoneutron stars and supernovae (Suzuki 1993; Hannestad & Raffelt 1998; Burrows et al. 2000; Thompson, Burrows, & Horvath 2000). Neutron–neutron, proton–proton, and neutron–proton bremsstrahlung are all important, with the latter the most important for symmetric matter. As a source of ν_e and $\bar{\nu}_e$ neutrinos, nucleon–nucleon bremsstrahlung can not compete with the charged–current capture processes. However, for a range of temperatures and densities realized in supernova cores, it may compete with e^+e^- annihilation as a source for ν_μ , $\bar{\nu}_\mu$, ν_τ , and $\bar{\nu}_\tau$ neutrinos (“ ν_μ ”s). The major obstacles to obtaining accurate estimates of the emissivity of this process are our poor knowledge of the nucleon–nucleon potential, of the degree of suitability of the Born Approximation, and of the magnitude of many–body effects (Hannestad & Raffelt 1998; Raffelt & Seckel 1998; Brinkmann & Turner 1988). Since the nucleons in protoneutron star atmospheres are not degenerate, we present here a calculation of the total and differential emissivities of this process in that limit and assume a one-pion exchange (OPE) potential model to calculate the nuclear matrix element. For the corresponding calculation for arbitrary nucleon degeneracy, the reader is referred to Thompson, Burrows, & Horvath (2000). The formalism we employ has been heavily influenced by those of Brinkman and Turner (1988) and Hannestad and Raffelt (1998), to which the reader is referred for details and further explanations.

Our focus is on obtaining a useful single-neutrino final-state emission (source) spectrum, as well as a final-state pair energy spectrum and the total emission rate. For this, we start with Fermi’s Golden Rule for the total rate per neutrino species:

$$Q_{nb} = (2\pi)^4 \int \left[\prod_{i=1}^4 \frac{d^3 \vec{p}_i}{(2\pi)^3} \right] \frac{d^3 \vec{q}_\nu}{(2\pi)^3 2\omega_\nu} \frac{d^3 \vec{q}_{\bar{\nu}}}{(2\pi)^3 2\omega_{\bar{\nu}}} \omega \sum_s |\mathcal{M}|^2 \delta^4(\mathbf{P}) \Xi_{brems},$$

where

$$\Xi_{brems} = \mathcal{F}_1 \mathcal{F}_2 (1 - \mathcal{F}_3) (1 - \mathcal{F}_4), \quad (116)$$

$\delta^4(\mathbf{P})$ is four-momentum conservation delta function, ω is the energy of the final-state neutrino pair, $(\omega_\nu, \vec{q}_\nu)$ and $(\omega_{\bar{\nu}}, \vec{q}_{\bar{\nu}})$ are the energy and momentum of the neutrino and anti-neutrino, respectively, and \vec{p}_i is the momentum of nucleon i . Final-state neutrino and anti-neutrino blocking have been dropped.

The necessary ingredients for the integration of eq. (116) are the matrix element for the interaction and a workable procedure for handling the phase space terms, constrained by the conservation laws. We follow Brinkman and Turner (1988) for both of these elements. In particular, we assume for the $n + n \rightarrow n + n + \nu \bar{\nu}$ process that the matrix element is:

$$\begin{aligned} \sum_s |\mathcal{M}|^2 &= \frac{64}{4} G^2 (f/m_\pi)^4 g_A^2 \left[\left(\frac{k^2}{k^2 + m_\pi^2} \right)^2 + \dots \right] \frac{\omega_\nu \omega_{\bar{\nu}}}{\omega^2} \\ &= A \frac{\omega_\nu \omega_{\bar{\nu}}}{\omega^2}, \end{aligned} \quad (117)$$

where the 4 in the denominator accounts for the spin average for identical nucleons, G is the weak coupling constant, f (~ 1.0) is the pion-nucleon coupling constant, g_A is the axial-vector coupling constant, the term in brackets is from the OPE propagator plus exchange and cross terms, k is the nucleon momentum transfer, and m_π is the pion mass. In eq. (117), we have dropped $\vec{q}_\nu \cdot \vec{k}$ terms from the weak part of the total matrix element. To further simplify the calculation, we set the “propagator” term equal to a constant ζ , a number of order unity, and absorb into ζ all interaction ambiguities.

Recently, Hanhart, Phillips, & Reddy (2001) have addressed these momentum terms in the context of axion emission and $\nu_\mu \bar{\nu}_\mu$ production in supernovae. In an effort to make contact with the approximation to the matrix element we present here, they plot ζ as a function of average relative thermal nucleon momentum (\bar{p} ; Phillips, private communication).

The function peaks for $\zeta(\bar{p})$ between 150 – 200 MeV at $\zeta \simeq 0.47$. At $\bar{p} = 50$ MeV $\zeta \simeq 0.08$ and at $\bar{p} = 500$ MeV $\zeta \simeq 0.27$. We are most interested in the region around the ν_μ neutrinospheres, where the emergent spectrum might be most affected by nucleon-nucleon bremsstrahlung. Mass densities and temperatures in this region might be $10^{12} - 10^{13}$ g cm^{-3} and 5 – 10 MeV, respectively. We estimate \bar{p} in this regime to be ~ 175 MeV and take $\zeta = 0.5$ for all thermodynamical points. The constant A in eq. (117) remains.

Inserting a $\int \delta(\omega - \omega_\nu - \omega_{\bar{\nu}})d\omega$ by the neutrino phase space terms times $\omega\omega_\nu\omega_{\bar{\nu}}/\omega^2$ and integrating over $\omega_{\bar{\nu}}$ yields:

$$\int \omega \frac{\omega_\nu\omega_{\bar{\nu}}}{\omega^2} \frac{d^3\vec{q}_\nu}{(2\pi)^3 2\omega_\nu} \frac{d^3\vec{q}_{\bar{\nu}}}{(2\pi)^3 2\omega_{\bar{\nu}}} \rightarrow \frac{1}{(2\pi)^4} \int_0^\infty \int_0^\omega \frac{\omega_\nu^2(\omega - \omega_\nu)^2}{\omega} d\omega_\nu d\omega, \quad (118)$$

where again ω equals $(\omega_\nu + \omega_{\bar{\nu}})$. If we integrate over ω_ν , we can derive the ω spectrum. A further integration over ω will result in the total volumetric energy emission rate. If we delay such an integration, after the nucleon phase space sector has been reduced to a function of ω and if we multiply eq. (116) and/or eq. (118) by ω_ν/ω , an integration over ω from ω_ν to infinity will leave the emission spectrum for the single final-state neutrino. This is of central use in multi-energy group transport calculations and with this differential emissivity and Kirchhoff's Law (§2) we can derive an absorptive opacity.

Whatever our final goal, we need to reduce the nucleon phase space integrals and to do this we use the coordinates and approach of Brinkman and Turner (1988). We define new momenta: $p_+ = (p_1 + p_2)/2$, $p_- = (p_1 - p_2)/2$, $p_{3c} = p_3 - p_+$, and $p_{4c} = p_4 - p_+$, where nucleons 1 and 2 are in the initial state. Useful direction cosines are $\gamma_1 = p_+ \cdot p_- / |p_+||p_-|$ and $\gamma_c = p_+ \cdot p_{3c} / |p_+||p_{3c}|$. Defining $u_i = p_i^2/2mT$ and using energy and momentum conservation, we can show that:

$$\begin{aligned} d^3p_1 d^3p_2 &= 8d^3p_+ d^3p_- \\ \omega &= 2T(u_- - u_{3c}) \\ u_{1,2} &= u_+ + u_- \pm 2(u_+ u_-)^{1/2} \gamma_1 \\ u_{3,4} &= u_+ + u_{3c} \pm 2(u_+ u_{3c})^{1/2} \gamma_c. \end{aligned} \quad (119)$$

In the non-degenerate limit, the $\mathcal{F}_1 \mathcal{F}_2 (1 - \mathcal{F}_3)(1 - \mathcal{F}_4)$ term reduces to $e^{2y} e^{-2(u_+ + u_-)}$, where y is the nucleon degeneracy factor. Using eq. (119), we see that the quantity $(u_+ + u_-)$ is independent of both γ_1 and γ_c . This is a great simplification and makes the angle integrations trivial. Annihilating d^3p_4 with the momentum delta function in eq.

(116), noting that $p_i^2 dp = \frac{(2mT)^{3/2}}{2} u_i^{1/2} du_i$, pairing the remaining energy delta function with u_- , and integrating u_+ from 0 to ∞ , we obtain:

$$dQ_{nb} = \frac{Am^{4.5}}{2^8 \times 3 \times 5\pi^{8.5}} T^{7.5} e^{2y} e^{-\omega/T} (\omega/T)^4 \left[\int_0^\infty e^{-x} (x^2 + x\omega/T)^{1/2} dx \right] d\omega. \quad (120)$$

The variable x over which we are integrating in eq. (120) is equal to $2u_{3c}$. That integral is analytic and yields:

$$\int_0^\infty e^{-x} (x^2 + x\omega/T)^{1/2} dx = \eta e^\eta K_1(\eta), \quad (121)$$

where K_1 is the standard modified Bessel function of imaginary argument, related to the Hankel functions, and $\eta = \omega/2T$. Hence, the ω spectrum is given by:

$$\frac{dQ_{nb}}{d\omega} \propto e^{-\omega/2T} \omega^5 K_1(\omega/2T). \quad (122)$$

It can easily be shown that $\langle \omega \rangle = 4.364T$. Integrating eq. (120) over ω and using the thermodynamic identity in the non-degenerate limit:

$$e^y = \left(\frac{2\pi}{mT} \right)^{3/2} n_n/2, \quad (123)$$

where n_n is the density of neutrons (in this case), we derive for the total neutron–neutron bremsstrahlung emissivity of a single neutrino pair:

$$Q_{nb} = 1.04 \times 10^{30} \zeta (X_n \rho_{14})^2 \left(\frac{T}{\text{MeV}} \right)^{5.5} \text{ ergs cm}^{-3} \text{ s}^{-1}, \quad (124)$$

where ρ_{14} is the mass density in units of 10^{14} gm cm $^{-3}$ and X_n is the neutron mass fraction. Interestingly, this is within 30% of the result in Suzuki (1993), even though he has substituted, without much justification, $(1 + \omega/2T)$ for the integral in eq. (120). ($[1 + (\pi\eta/2)^{1/2}]$ is a better approximation.) The proton–proton and neutron–proton processes can be handled similarly and the total bremsstrahlung rate is then obtained by substituting $X_n^2 + X_p^2 + \frac{28}{3} X_n X_p$ for X_n^2 in eq. (124) (Brinkmann and Turner 1988). At $X_n = 0.7$, $X_p = 0.3$, $\rho = 10^{12}$ gm cm $^{-3}$, and $T = 10$ MeV, and taking the ratio of augmented eq. (124) to eq. (105), we obtain the promising ratio of $\sim 5\zeta$. Setting the correction factor ζ equal to ~ 0.5 (Hanhart, Phillips, and Reddy 2001), we find that near and just deeper than the ν_μ neutrinosphere, bremsstrahlung is larger than classical pair production.

If in eq. (118) we do not integrate over ω_ν , but at the end of the calculation we integrate over ω from ω_ν to ∞ , after some manipulation we obtain the single neutrino emissivity spectrum:

$$\frac{dQ'_{nb}}{d\omega_\nu} = 2C \left(\frac{Q_{nb}}{T^4} \right) \omega_\nu^3 \int_{\eta_\nu}^{\infty} \frac{e^{-\eta}}{\eta} K_1(\eta) (\eta - \eta_\nu)^2 d\eta \quad (125)$$

$$= 2C \left(\frac{Q_{nb}}{T^4} \right) \omega_\nu^3 \int_1^{\infty} \frac{e^{-2\eta_\nu \xi}}{\xi^3} (\xi^2 - \xi)^{1/2} d\xi, \quad (126)$$

where $\eta_\nu = \omega_\nu/2T$, C is the normalization constant equal to $\frac{3 \times 5 \times 7 \times 11}{2^{11}}$ ($\cong 0.564$), and for the second expression we have used the integral representation of $K_1(\eta)$ and reversed the order of integration. In eq. (126), Q_{nb} is the emissivity for the pair.

Eq. (126) is the approximate neutrino emission spectrum due to nucleon–nucleon bremsstrahlung. A useful fit to eq. (126), good to better than 3% over the full range of important values of η_ν , is:

$$\frac{dQ'_{nb}}{d\omega_\nu} \cong \frac{0.234 Q_{nb}}{T} \left(\frac{\omega_\nu}{T} \right)^{2.4} e^{-1.1\omega_\nu/T}. \quad (127)$$

Thompson, Burrows, and Horvath (2000) should be consulted for a detailed discussion of nucleon-nucleon bremsstrahlung for arbitrary nucleon degeneracy.

9. Conclusion

The processes that have been described above are essential elements of the neutrino-driven supernova explosion mechanism. Coupling these with radiation-hydrodynamics codes, an equation of state, beta-decay and electron capture microphysics, and nuclear rates, one explores the viability of various scenarios for the explosion of the cores of massive stars (Liebendörfer et al. 2001ab; Rampp & Janka 2000). Recently, Thompson, Burrows, and Pinto (2002) have incorporated this neutrino microphysics into simulations of 1D (spherical) core collapse and have investigated the effects on the dynamics, luminosities, and emergent spectra of weak magnetism/recoil, nucleon-nucleon bremsstrahlung, inelastic neutrino-electron scattering, and a host of the cross section corrections described above. Figures 8 and 9 depict some of the resultant luminosity spectra and their temporal evolution for a representative simulation. The character of the spectra reflect the opacities and sources described in this paper. In particular, the energy hardness hierarchy from ν_e (softer) to ν_μ (harder) neutrinos is clearly demonstrated on these plots, as is

the distinction between the ν_e pre-breakout and post-breakout spectra (Fig. 8). (See the figure captions for further details.)

To date, none of the detailed 1D simulations that have been performed explodes and it may be that multi-dimensional effects play a pivotal role in the explosion mechanism (Herant et al. 1994; Burrows, Hayes, & Fryxell 1995; Fryer et al. 1999; Janka & Müller 1996). Be that as it may, an understanding of neutrino-matter interactions remains central to unraveling one of the key mysteries of the nuclear universe in which we live.

Acknowledgments

We would like to thank Ray Sawyer, Sanjay Reddy, and Jorge Horvath for fruitful discussions and/or collaboration on some of the more thorny aspects of neutrino-matter interactions. Support for this work was provided by the Scientific Discovery through Advanced Computing (SciDAC) program of the DOE, grant number DE-FC02-01ER41184, and by NASA through Hubble Fellowship grant #HST-HF-01157.01-A awarded by the Space Telescope Science Institute, which is operated by the Association of Universities for Research in Astronomy, Inc., for NASA, under contract NAS 5-26555.

References

- Aufderheide, M., Fushiki, I., Fuller, G., and Weaver, T. 1994, *Ap. J.*, 424, 257
 Backman, S.-O., Brown, G.E., & Niskanen, J.A. 1985, *Physics Reports*, 124, 1
 Bowers, R. L. & Wilson, J. R. 1982, *ApJS*, 50, 115
 Brinkmann, R. P. & Turner, M. S. 1988, *Phys. Rev. D*, 38, 8, 2338
 Brown, G.E. & Rho, M. 1981, *Nucl. Phys.*, A 372, 397
 Bruenn, S. W. 1985, *ApJS*, 58, 771
 Bruenn, S.W. and A. Mezzacappa 1997, *Phys. Rev. D*, 56, 7529
 Buras, R., Janka, H.-Th., Keil, M. Th., & Raffelt, G. G., Rampp, M. 2002, submitted to *ApJ*, (astro-ph/0205006)
 Burrows, A., Mazurek T. J., & Lattimer, J. M. 1981, *ApJ*, 251, 325
 Burrows, A., Hayes, J., & Fryxell, B. A. 1995, *ApJ*, 450, 830
 Burrows, A. and Sawyer, R.F. 1998, *Phys. Rev. C*, 58, 554
 Burrows, A. and Sawyer, R.F. 1999, *Phys. Rev. C*, 59, 510
 Burrows, A. 2000, *Nature*, 403, 727
 Burrows, A., Young, T., Pinto, P.A., Eastman, R., and Thompson, T. 2000, *Ap. J.*, 539, 865
 Dicus, D.A. 1972, *Phys. Rev. D*, 6, 941
 Fetter, A.L. & Walecka, J.D. 1971, *Quantum Theory of Many Particle Systems* (New York: McGraw-Hill)
 Flowers, E., Sutherland, P., and Bond, J.R. 1975, *Phys. Rev. D*, 12, 316
 Freedman, D.Z. 1974, *Phys. Rev. D*, 9, 1389

- Fryer, C. L., Benz, W., Herant, M., & Colgate, S. 1999, ApJ, 516, 892
- Fuller, G. 1982, *Ap. J.*, 252, 741
- Fuller, G. M., Fowler, W. A., & Newman, M. J. 1982, ApJ, 252, 715
- Hanhart, C., Phillips, D. & Reddy, S. 2001, Phys. Lett. B, 499, 9
- Hannestad, S. and Raffelt, G. 1998, *Ap. J.*, 507, 339
- Herant, M., Benz, W., Hix, W. R., Fryer, C. L., Colgate, S. A. 1994, ApJ, 435, 339
- Horowitz, C. J. 1997, Phys. Rev. D, 55, no. 8
- Horowitz, C. J. 2002, Phys Rev. D, 65, 043001
- Janka, H.-T. 1991, *Astr. Ap.*, 244, 378
- Janka, H.-Th. & Müller, E. 1996, A&A, 306, 167
- Janka, H.-T., Keil, W., Raffelt, G., and Seckel, D. 1996, *Phys. Rev. Lett.*, 76, 2621
- Lamb, D. & Pethick, C. 1976, ApJL, 209, L77
- Landau, L.D. and Lifschitz, E.M. 1969, *Statistical Physics*, 2nd edition (Pergamon Press; New York) p.352
- Leinson, L.B., Oraevsky, V.N., & Semikoz, V.B. 1988, Phys. Lett. B, 209, 1
- Liebendörfer, M., Mezzacappa, A., Thielemann, F.-K., Messer, O. E. B., Hix, W. R., & Bruenn, S. W. 2001, PRD, 63, 103004
- Liebendörfer, M., Mezzacappa, A., Thielemann, F.-K. 2001, PRD, 63, 104003
- Mezzacappa, A. & Bruenn, S. W. 1993a, ApJ, 410, 637
- Mezzacappa, A. & Bruenn, S. W. 1993b, ApJ, 410, 669
- Mezzacappa, A. & Bruenn, S. W. 1993c, ApJ, 410, 740
- Raffelt, G. & Seckel, D. 1998, Phys. Rev. Lett., 69, 2605
- Raffelt, G. 2001, ApJ, 561,890
- Rampp, M. & Janka, H.-Th. 2000, ApJL, 539, 33
- Reddy, S., Prakash, M., & Lattimer, J. M. 1998, PRD, 58, 013009
- Schinder, P.J. 1990, ApJS, 74, 249
- Smit, J.M. 1998, Ph.D. Thesis, Universiteit van Amsterdam
- Smit, J.M. & Cernohorsky, J. 1996, A&A, 311, 347
- Suzuki, H. in *Frontiers of Neutrino Astrophysics*, ed. Suzuki, Y. & Nakamura, K. 1993, (Tokyo: Universal Academy Press), 219
- Thompson, T. A., Burrows, A., & Horvath, J. E. 2000, PRC, 62, 035802
- Thompson, T. A., Burrows, A., & Pinto, P.A. 2002, in preparation
- Tubbs, D. L. & Schramm, D. N. 1975, ApJ, 201, 467
- Vogel, P. 1984, Phys. Rev. D, 29, 1918
- Yamada, S., Janka, H.-T., and Suzuki, H. 1999, *Astr. Ap.*, 344, 533

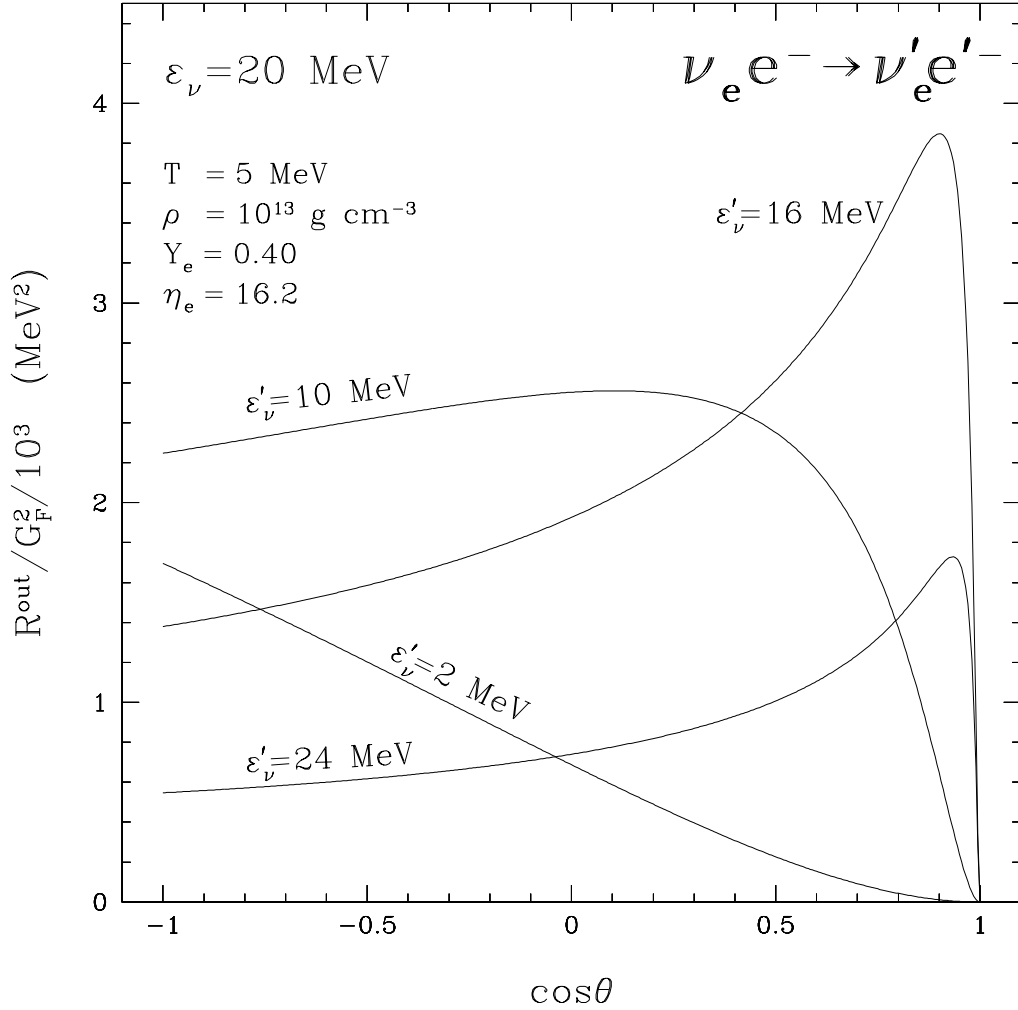


Figure 1. The scattering kernel $R^{\text{out}}(\varepsilon_\nu, \varepsilon'_\nu, \cos\theta)$ for ν_e -electron scattering as a function of $\cos\theta$ for $\varepsilon_\nu = 20 \text{ MeV}$ and $\varepsilon'_\nu = 2, 10, 16,$ and 24 MeV , at a representative thermodynamic point ($T = 5 \text{ MeV}$, $\rho = 10^{13} \text{ g cm}^{-3}$, $Y_e = 0.4$).

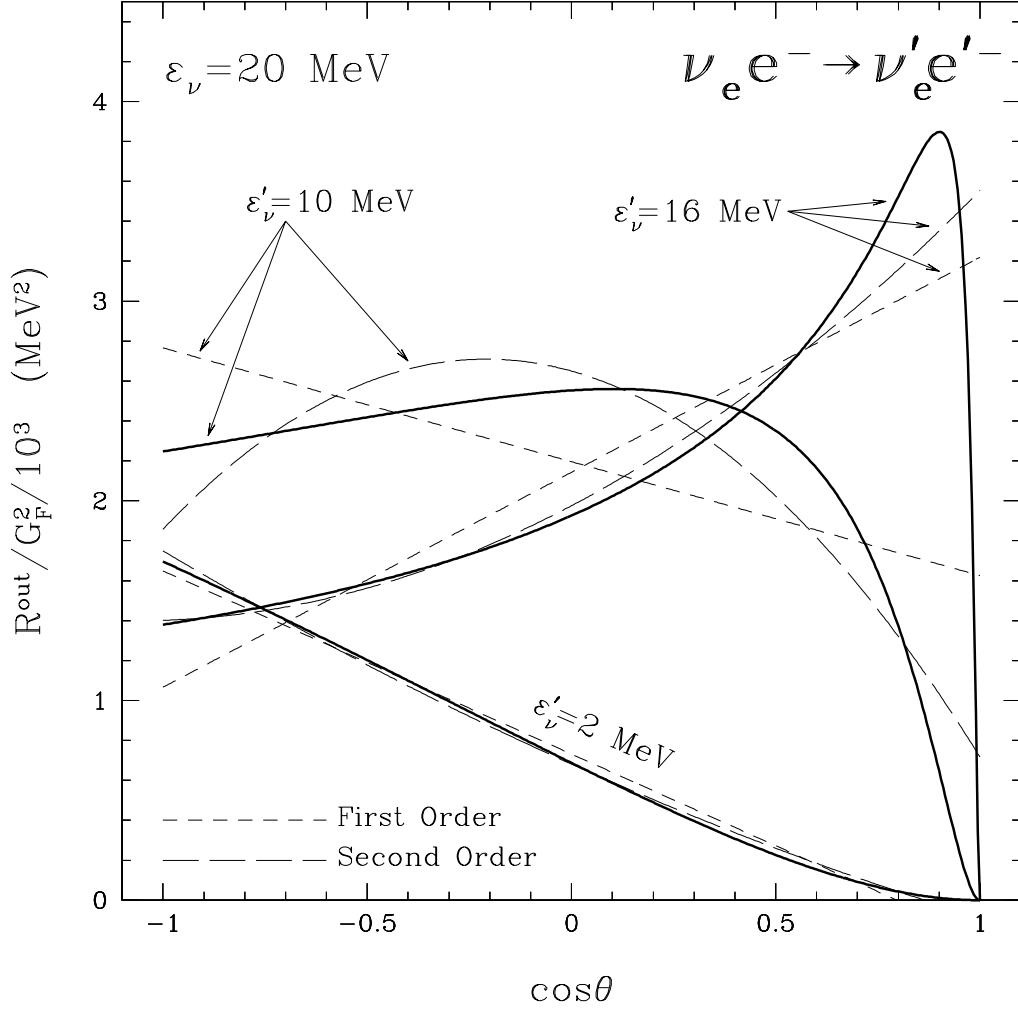


Figure 2. For the same thermodynamic point as used for Fig. (1), the scattering kernel (R^{out} , thick solid lines) for ν_e -electron scattering as a function of $\cos \theta$, for $\varepsilon_\nu = 20$ MeV and $\varepsilon'_\nu = 2, 10,$ and 16 MeV. Short dashed lines show the first-order Legendre series expansion approximation to R^{out} , which is linear in $\cos \theta$; $R^{\text{out}} \sim (1/2)\Phi_0 + (3/2)\Phi_1 \cos \theta$. The long dashed line shows the improvement in going to second order in $\cos \theta$ by taking $R^{\text{out}} \sim (1/2)\Phi_0 + (3/2)\Phi_1 \cos \theta + (5/2)\Phi_2(1/2)(3 \cos^2 \theta - 1)$.

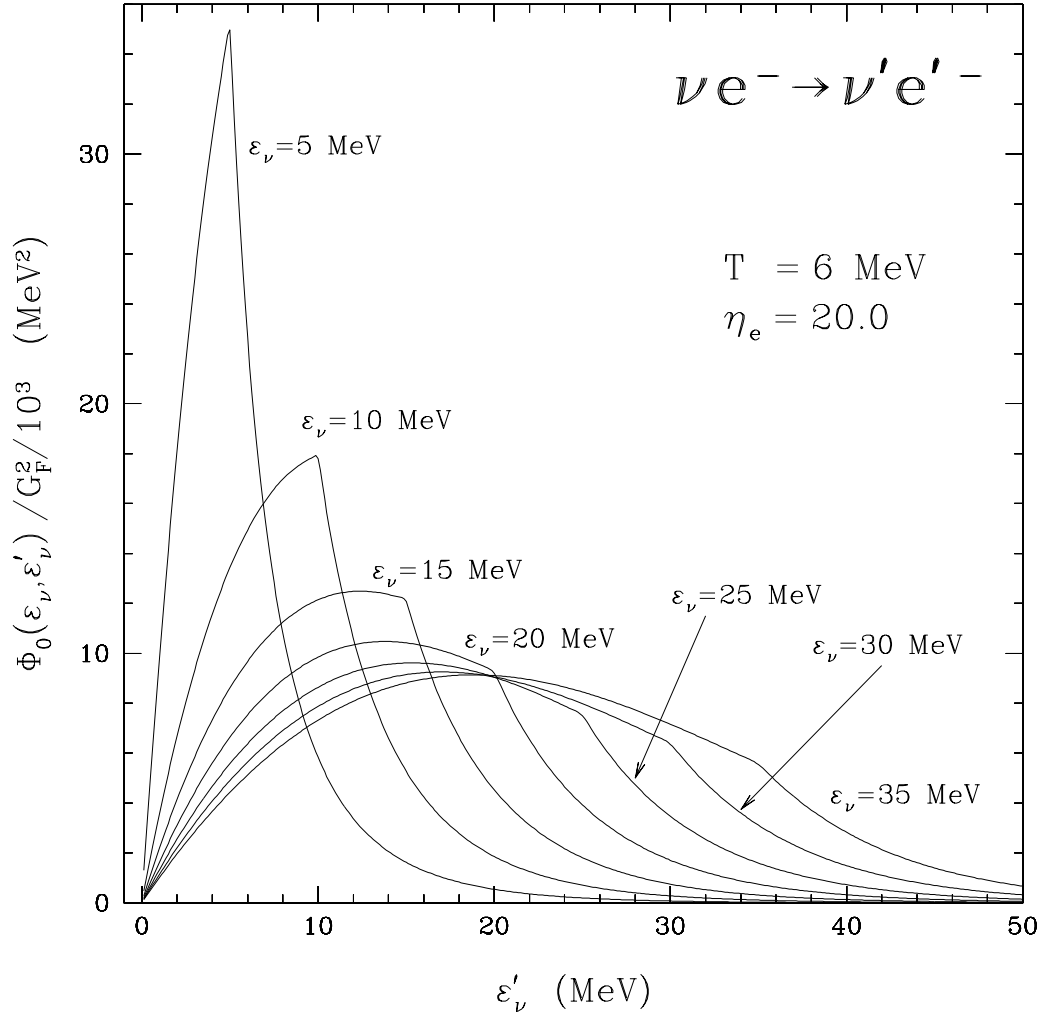


Figure 3. The $l = 0$ term in the Legendre expansion of the ν_e -electron scattering kernel, $\Phi_0(\varepsilon_\nu, \varepsilon'_\nu)$ (eq. 38), for $T = 6$ MeV and $\eta_e = 20$ as a function of ε'_ν for $\varepsilon_\nu = 5, 10, 15, 20, 25,$ and 35 MeV. Note that for any ε_ν , the neutrino is predominantly downscattered. The magnitude of $\Phi_0(\varepsilon_\nu, \varepsilon'_\nu)$ and sign of $\langle \omega \rangle$ are to be compared with those in Fig. (5).

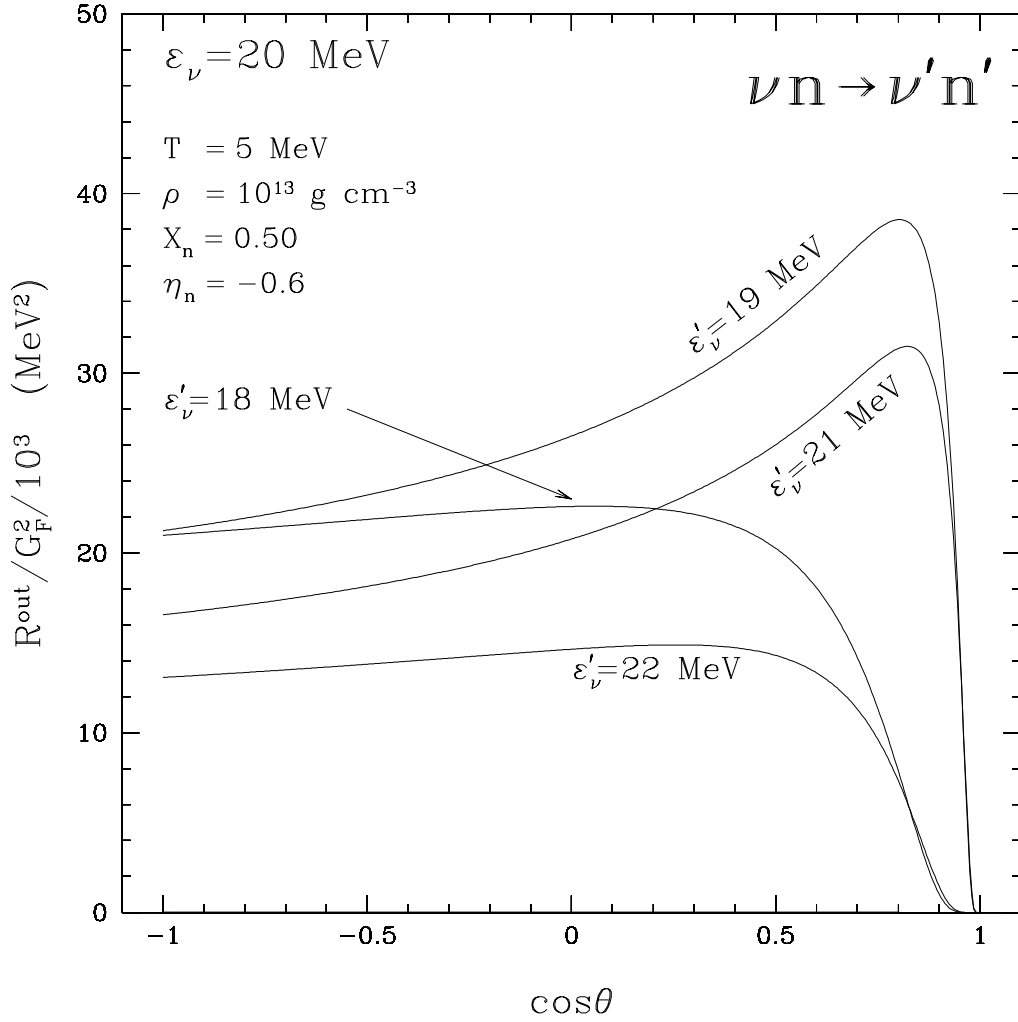


Figure 4. The scattering kernel $R^{\text{out}}(\varepsilon_\nu, \varepsilon'_\nu, \cos\theta)$ for ν_e -neutron scattering as a function of $\cos\theta$ for $\varepsilon_\nu = 20$ MeV and $\varepsilon'_\nu = 18, 19, 21,$ and 22 MeV, at a representative thermodynamic point ($T = 5$ MeV, $\rho = 10^{13}$ g cm $^{-3}$, $X_n = 0.5$). Note that although the absolute value of the energy transfer ($|\varepsilon_\nu - \varepsilon'_\nu|$) is the same for both $\varepsilon'_\nu = 19$ MeV and $\varepsilon'_\nu = 21$ MeV, the absolute value of $R^{\text{out}}(20, 19, \cos\theta)$ is greater than that of $R^{\text{out}}(20, 21, \cos\theta)$, reflecting the fact that at this temperature the incoming neutrino is more likely to downscatter than upscatter.

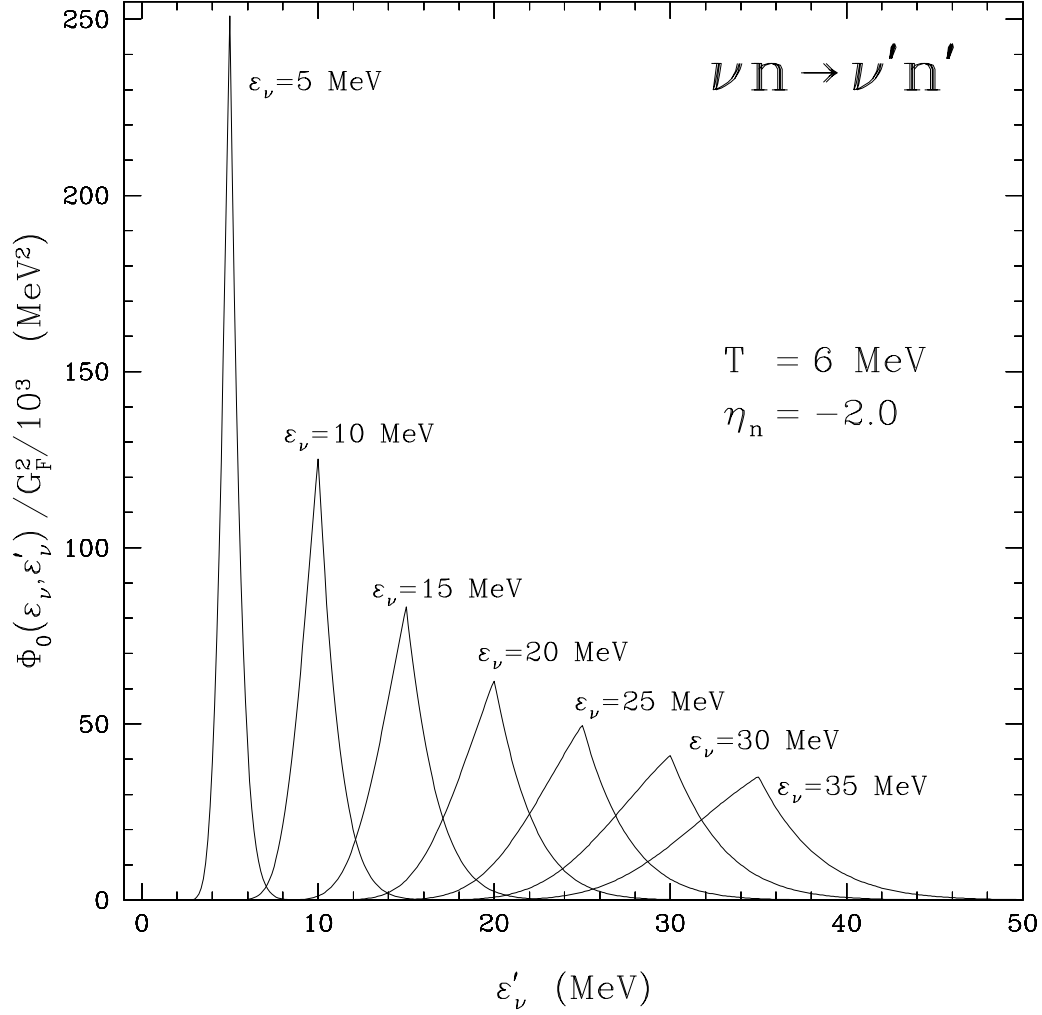


Figure 5. The $l = 0$ term in the Legendre expansion of the neutrino-nucleon scattering kernel, $\Phi_0(\varepsilon_\nu, \varepsilon'_\nu)$ (eq. 38), for $T = 6$ MeV and $\eta_n = -2$ as a function of ε'_ν for $\varepsilon_\nu = 5, 10, 15, 20, 25,$ and 35 MeV. Note that for $\varepsilon_\nu = 5$ MeV the neutrino is predominantly upscattered, while for $\varepsilon_\nu = 35$ MeV the neutrino is predominantly downscattered. The magnitude of $\Phi_0(\varepsilon_\nu, \varepsilon'_\nu)$ and sign of $\langle \omega \rangle$ are to be compared with those in Fig. (3).

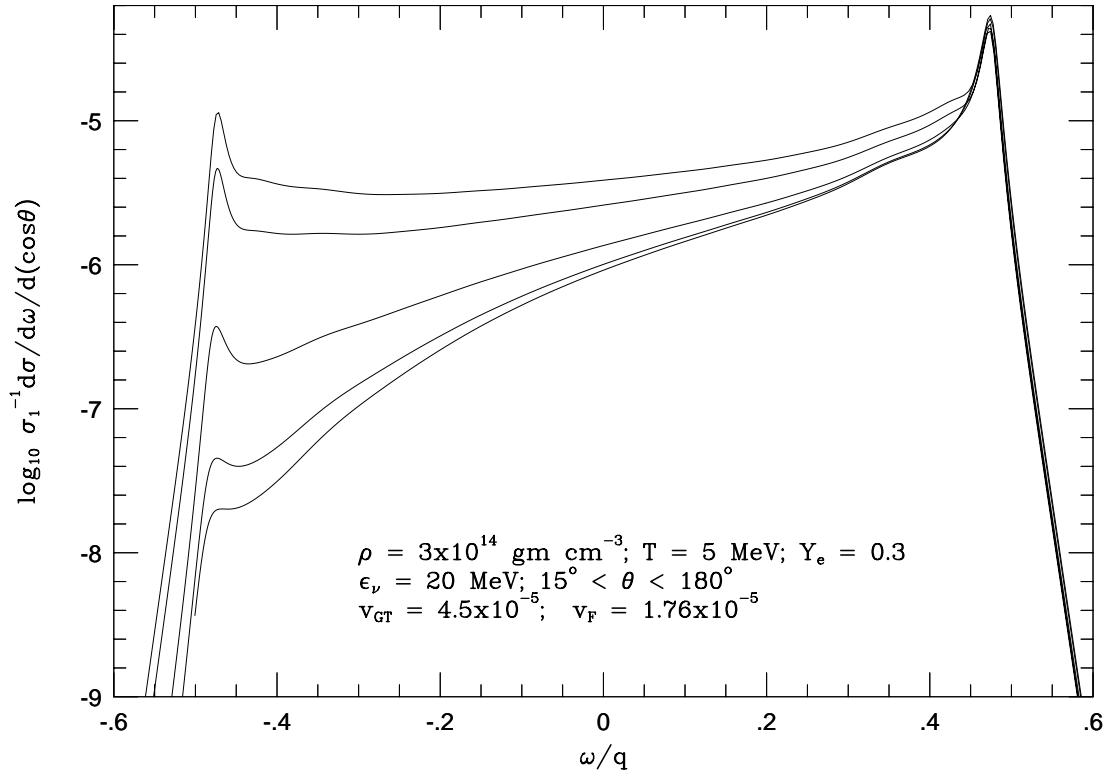


Figure 6. Log_{10} of the doubly-differential cross section for neutral-current neutrino-nucleon scattering versus ω/q for scattering angles 15° , 45° , 90° , 135° , and 180° . The calculations were performed at a temperature of 5 MeV, a Y_e of 0.3, a ρ of $3 \times 10^{14} \text{ g cm}^{-3}$, and an incident neutrino energy of 20 MeV. The default potentials ($v_{GT} = 4.5 \times 10^{-5}$ and $v_F = 1.76 \times 10^{-5}$) and effective mass ($m^* = 0.75 m_n$) were employed. The differential cross section is divided by the total scattering cross section (σ_1) in the non-interacting, no-nucleon-blocking, $\omega = 0$ limit. (Figure taken from Burrows and Sawyer 1998.)

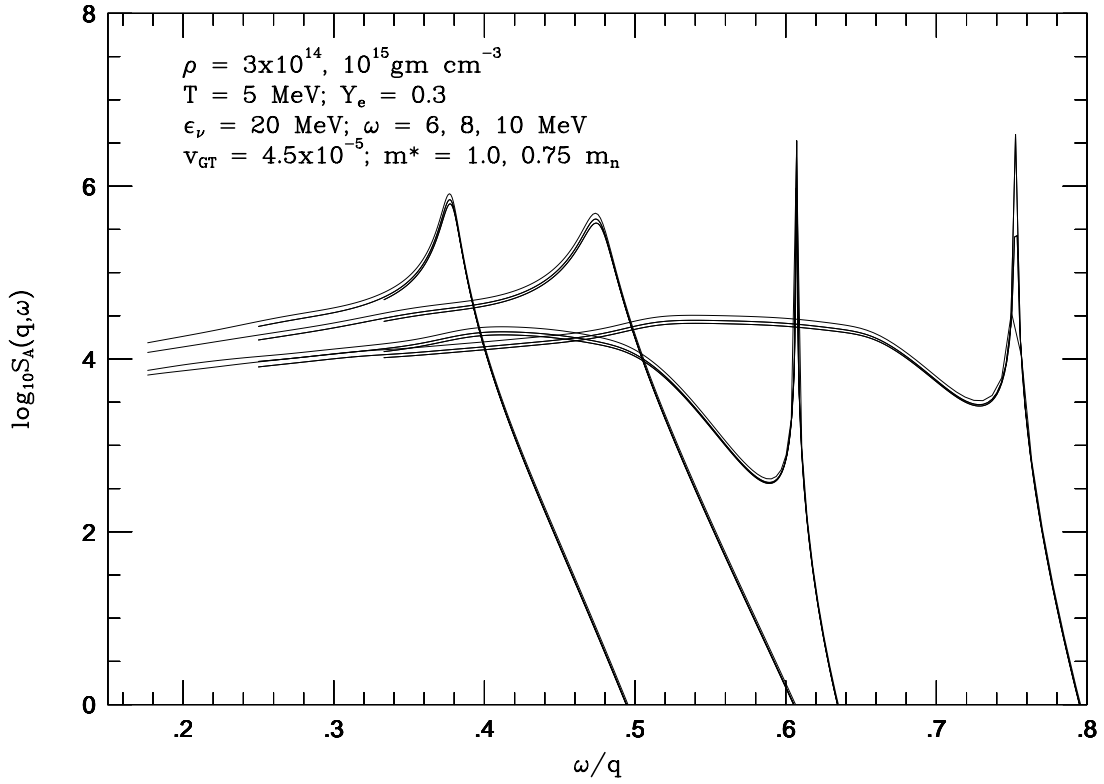


Figure 7. \log_{10} of the Gamow–Teller structure function versus ω/q for an incident neutrino energy of 20 MeV, energy transfers, ω , of 6, 8, and 10 MeV, two values of the effective mass ($m^* = [0.75m_n, 1.0m_n]$) and two values of the density ($\rho = 3 \times 10^{14}$ and $10^{15} \text{ g cm}^{-3}$). A temperature of 5 MeV and a Y_e of 0.3 were used, as was the default v_{GT} ($= 4.5 \times 10^{-5}$). (Figure taken from Burrows and Sawyer 1998.)

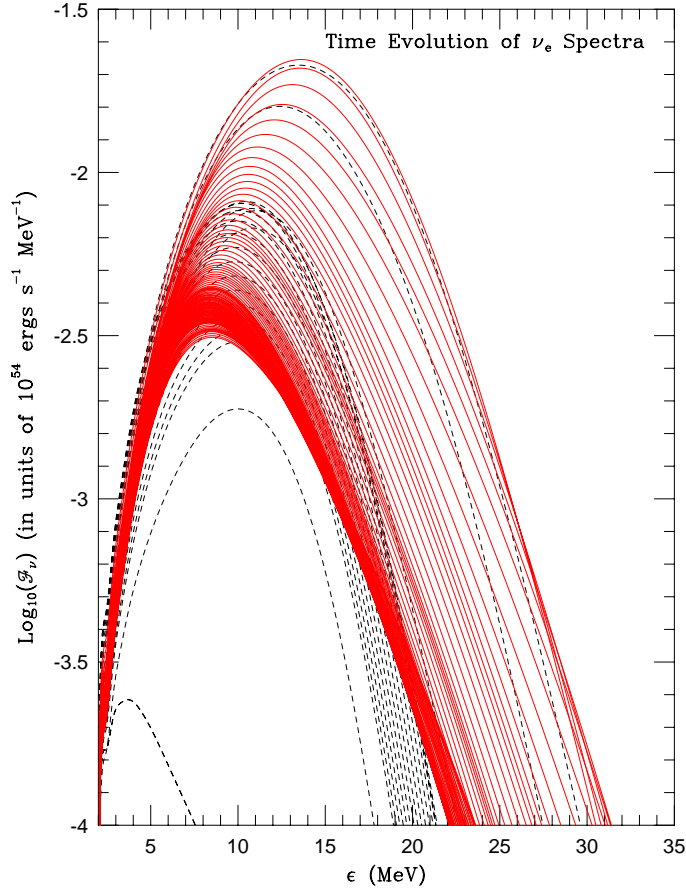


Figure 8. A collection of emergent ν_e spectra at various times during the core-collapse, bounce, and shock-stagnation phases of the core of an $11 M_{\odot}$ progenitor. The luminosity spectrum (logarithm base ten) is in units of $10^{54} \text{ ergs s}^{-1} \text{ MeV}^{-1}$ and the neutrino energy (abscissa) is in units of MeV. The dashed curves cover the collapse phase (of duration ~ 200 milliseconds) until just before the peak luminosity around shock breakout is achieved and the solid curves are for the subsequent cooling and deleptonization phases after the peak. The last curve is at ~ 110 milliseconds after bounce. The lowest dashed curve is at a time early during collapse. Note the relative softness of the spectrum then. As the figure shows, the transition from the dashed to the solid curve happens close to the time when the ν_e spectrum is hardest.

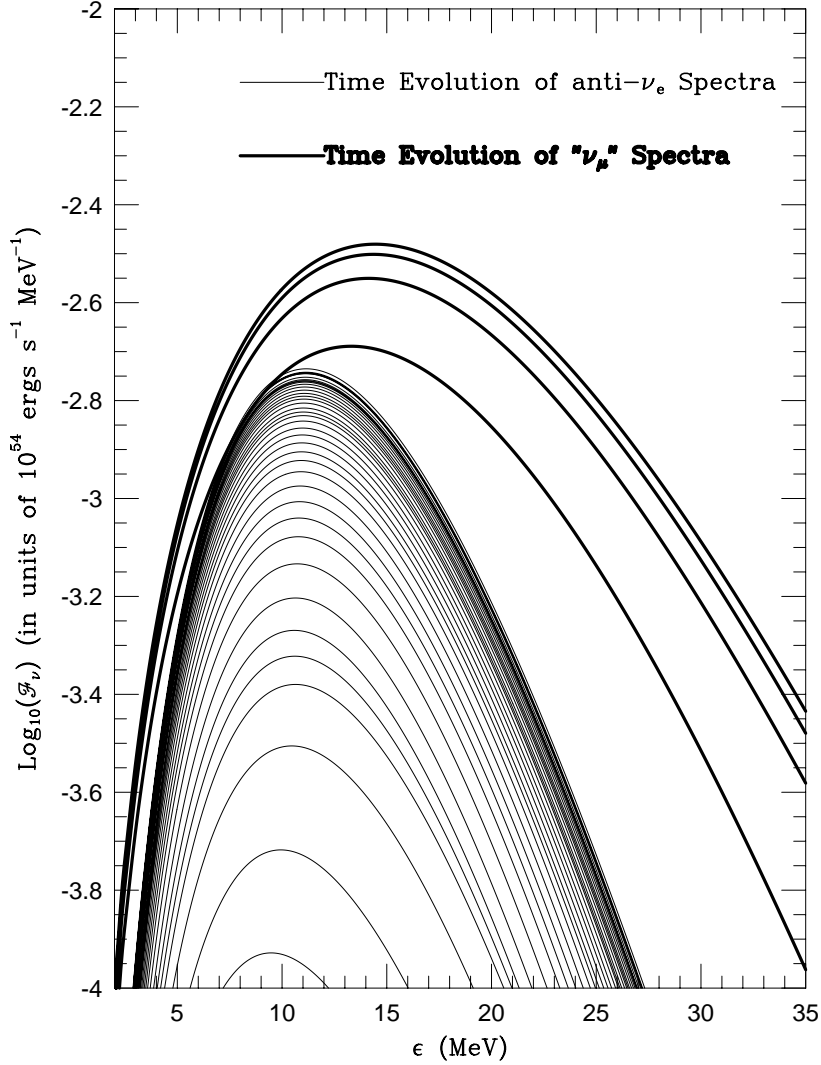


Figure 9. This figure shows the $\bar{\nu}_e$ (thin lines) and " ν_μ " (thick lines) emergent luminosity spectra for the $11 M_\odot$ progenitor evolution depicted in Fig. 8. The luminosity spectra (logarithm base ten) are in units of $10^{54} \text{ ergs s}^{-1} \text{ MeV}^{-1}$ and the neutrino energy (abscissa) is in units of MeV. There is no appreciable flux prior to shock breakout for these species. To avoid clutter, we here depict only a few ν_μ spectra to ~ 50 milliseconds after bounce. (These curves represent the sum of the ν_μ , $\bar{\nu}_\mu$, ν_τ , and $\bar{\nu}_\tau$ luminosity spectra.) However, the $\bar{\nu}_e$ spectra are shown until about 110 milliseconds after bounce. During the phases shown, both sets of luminosities are always increasing. Note that the ν_μ spectra are significantly harder than either the $\bar{\nu}_e$ or the ν_e spectra. This is a consequence of the fact that the ν_μ s do not have appreciable charged-current cross sections (eqs. 10 and 11), enabling one to probe more deeply into the hot core with these species.